Experimental Neurology 322 (2019) 113036

Contents lists available at ScienceDirect

Experimental Neurology

journal homepage: www.elsevier.com/locate/yexnr

Research paper

Acute L-DOPA administration reverses changes in firing pattern and low frequency oscillatory activity in the entopeduncular nucleus from long term L-DOPA treated 6-OHDA-lesioned rats

A. Aristieta[a,*,1], J.A. Ruiz-Ortega[a,b,c], T. Morera-Herreras[a,c], C. Miguelez[a,c], L. Ugedo[a,c]

[a] Department of Pharmacology, Faculty of Medicine and Dentistry, University of the Basque Country (UPV/EHU), 48940 Leioa, Spain
[b] Department of Pharmacology, Faculty of Pharmacy, University of the Basque Country (UPV/EHU), 01006 Vitoria-Gasteiz, Spain
[c] Autonomic and Movement Disorders Unit, Neurodegenerative Diseases, Biocruces Health Research Institute, Barakaldo, Spain

ARTICLE INFO

Keywords:
Parkinson's disease
Dyskinesia
Entopeduncular nucleus
L-DOPA
Subthalamic nucleus
Low oscillatory activity
6-OHDA
Basal ganglia
Electrophysiology
In vivo

ABSTRACT

The pathophysiology of Parkinson's disease (PD) and L-DOPA-induced dyskinesia (LID) is associated with aberrant neuronal activity and abnormal high levels of oscillatory activity and synchronization in several basal ganglia nuclei and the cortex. Previously, we have shown that the firing activity of neurons in the *substantia nigra pars reticulata* (SNr) is relevant in dyskinesia and may be driven by subthalamic nucleus (STN) hyperactivity. Conversely, low frequency oscillatory activity and synchronization in these structures seem to be more important in PD because they are not influenced by prolonged L-DOPA administration. The aim of the present study was to assess (through single-unit extracellular recording techniques under urethane anaesthesia) the neuronal activity of the entopeduncular nucleus (EPN) and its relationship with LID and STN hyperactivity, together with the oscillatory activity and synchronization between these nuclei and the cerebral cortex in 6-OHDA-lesioned rats that received long term L-DOPA treatment (or not). Twenty-four hours after the last L-DOPA injection the firing activity of EPN neurons in long term L-DOPA treated 6-OHDA-lesioned rats was more irregular and bursting compared to sham rats, being those alterations partially reversed by the acute challenge of L-DOPA. No correlation between EPN neurons firing activity and abnormal involuntary movements score was found. However, there was a significant correlation between the firing activity parameters of EPN and STN neurons recorded from long term L-DOPA treated 6-OHDA-lesioned rats. Low frequency oscillatory activity and synchronization both within the EPN and with the cerebral cortex were enhanced in 6-OHDA-lesioned animals. These changes were reversed by the acute L-DOPA challenge only in long term L-DOPA treated 6-OHDA-lesioned rats. Altogether, these results obtained from long term L-DOPA treated 6-OHDA-lesioned rats suggest (1) a likely relationship between STN and EPN firing patterns and spiking phases induced by changes after prolonged L-DOPA administration and (2) that the effect of L-DOPA on the firing pattern, low frequency oscillatory activity and synchronization in the EPN may have a relevant role in LID.

1. Introduction

Pharmacological replacement of dopamine (DA) with its precursor L-3,4-dihydroxyphenylalanine (L-DOPA) is the gold standard treatment for Parkinson's disease (PD). However, long-term administration of L-DOPA induces abnormal involuntary movements (AIMs) known as L-DOPA-induced dyskinesia (LID). These motor complications are potentially disabling, and affect up to 40% of PD patients within 5 years of treatment (Ahlskog and Muenter, 2001). Altered neural activity and abnormally synchronized oscillatory activity at multiple levels of the cortico-basal ganglia (BG) loop have been linked to motor dysfunction in PD patients with or without LID (Alonso-Frech et al., 2006; Fogelson et al., 2006; Kühn et al., 2006; Lozano et al., 2000; Obeso et al., 2000). Indeed, it has been suggested that the reversion of these alterations may be the target for therapeutic strategies in PD (Hammond et al., 2007). In PD patients, abnormal oscillatory activities are found at different

* Corresponding author at: Université de Bordeaux, Institut des Maladies Neurodégénératives, UMR 5293, 33076 Bordeaux, France. Centre National de la Recherche Scientifique, Institut des Maladies Neurodégénératives, UMR 5293, 33076 Bordeaux, France.
E-mail address: asier.aristieta@ehu.eus (A. Aristieta).
[1] Present address: Université de Bordeaux, Institut des Maladies Neurodégénératives, UMR 5293, 33076 Bordeaux, France. Centre National de la Recherche Scientifique, Institut des Maladies Neurodégénératives, UMR 5293, 33076 Bordeaux, France.

https://doi.org/10.1016/j.expneurol.2019.113036
Received 27 March 2019; Received in revised form 12 August 2019; Accepted 14 August 2019
Available online 16 August 2019

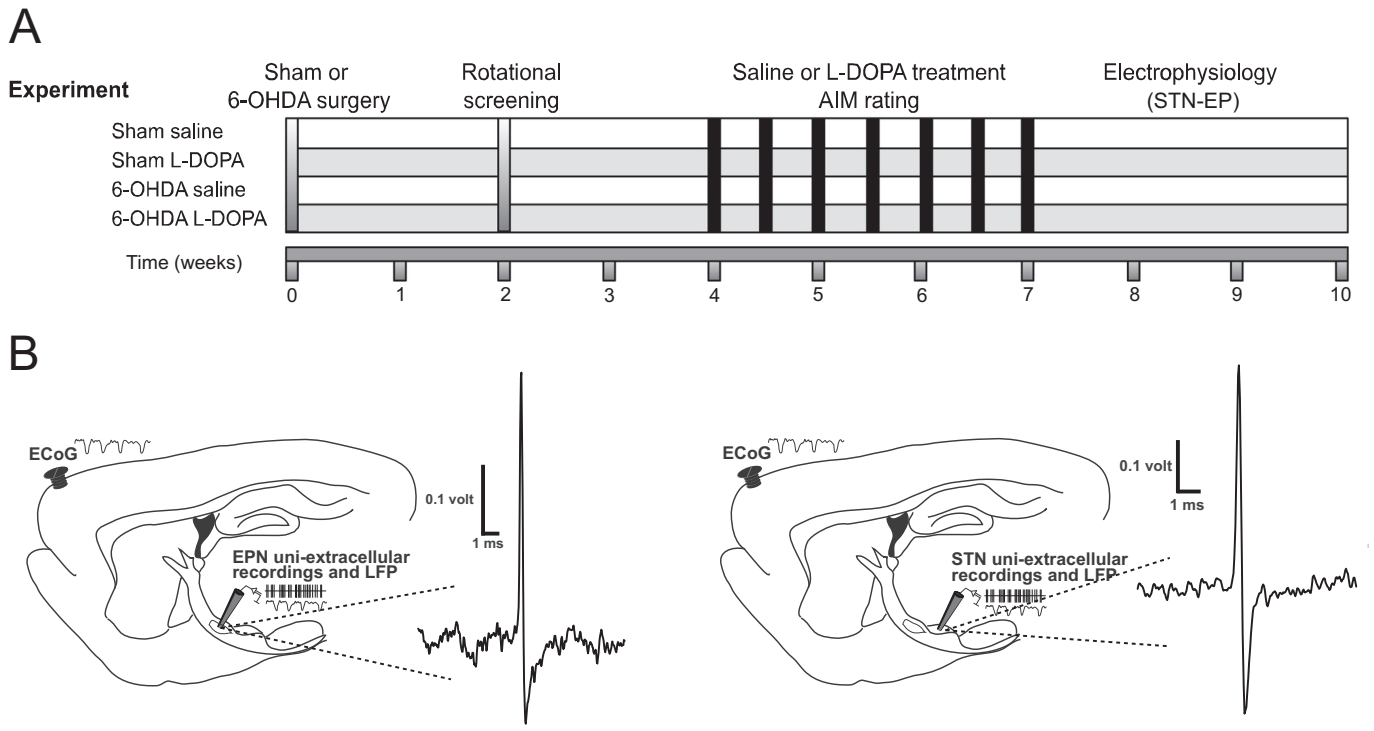

Fig. 1. Schematic representation of the experimental design and recording site. ***(A)*** At the beginning of the study, animals received a vehicle or 6-OHDA injection into the right medial forebrain bundle and were screened by amphetamine-induced rotations 2 weeks later. Rats were treated daily with saline or L-DOPA injections (6 mg/kg plus 12 mg/kg benserazide) for 21 days. AIMs were rated 2–3 days per week (testing sessions are marked in black). After the chronic treatment was completed, L-DOPA was administered twice per week, and electrophysiological experiments in STN and EPN were performed. All animals were perfused transcardially and processed for histology. ***(B)*** Schematic parasagittal section of a rat brain, showing the cortex and the BG nuclei. Glass electrodes were placed in the STN (Subthalamic nucleus, right) or the EPN (Entopeduncular nucleus, left) for recording single-unit extracellular activity and LFP. For recording the ECoG, a steel screw was implanted in the somatic sensory-motor cortex. A single spike from STN ***(B right)*** and EPN ***(B left)*** neurons recorded in vivo.

frequency ranges, including low frequency oscillations that have been associated with parkinsonian tremor (Smirnov et al., 2008; Tass et al., 2010), essential tremor (Tan et al., 2019), the expression of dyskinesia (Alonso-Frech et al., 2006), clinical improvement after L-DOPA intake (Giannicola et al., 2013) and pathological gambling in PD (Rosa et al., 2013).

One of the most often used PD animal model is the 6-hydroxydopamine (6-OHDA)-lesioned rodent. The injection of 6-OHDA into the nigrostriatal system induces degeneration of DA neurons in the *substantia nigra pars compacta* (SNc), and subsequently DA depletion in the striatum. This neurodegenerative process leads to the aberrant neuronal activity and the abnormal oscillatory activity that resemble those observed in PD patients (Mallet et al., 2008). Moreover, in 6-OHDA-lesioned rodents the prolonged L-DOPA treatment induces some molecular and behavioural alterations that emulate the LID observed in patients (Cenci et al., 1998). Thus, in this model of LID, it has been reported that the activity of the BG output nuclei, the *substantia nigra pars reticulata* (SNr) and the internal segment of the *globus pallidus* (GPi) (homologous to the entopeduncular nucleus (EPN) of rodents) is reduced (Aristieta et al., 2016; Boraud et al., 1998; Jin et al., 2016; Lacombe et al., 2009; Meissner et al., 2006). In addition, different frequency oscillatory activities, which may be detected under urethane anaesthesia (Magil et al., 2000; Tseng et al., 2001) are aberrantly presented in several BG nuclei (Aristieta et al., 2016; Mallet et al., 2008; Meissner et al., 2006; Parr-Brownlie et al., 2007; Walters et al., 2007) including the GPi/EPN (Jin et al., 2016). The GPi/EPN is a complex structure which participates in several physiological and pathological processes including motor control and sensory information processing (Shabel et al., 2012; Shabel et al., 2014; Wallace et al., 2017). Indeed, the GPi/EPN sends inhibitory GABAergic projections to several thalamic nuclei contributing to movement initiation and organization as well as action selection (Horak and Anderson, 1984; Mink, 1996; Redgrave et al., 1999). On the other hand, clinical evidences support the implication of the GPi in PD and LID since the lesion or the electrical high frequency stimulation of the GPi improves both motor impairment and particularly dyskinesia in humans (Olanow et al., 2000).

Previously we described that long term L-DOPA treated 6-OHDA-lesioned rats show important modifications of SNr firing activity which may be driven by the STN hyperactivity. Additionally, we also observed that the 6-OHDA lesion increases low frequency oscillatory activity in the STN and SNr, and that the chronic L-DOPA treatment does not change these augmented oscillations in urethane anaesthetized rats (Aristieta et al., 2016). However, the effect of the 6-OHDA lesion and the chronic L-DOPA treatment on the other less studied BG output structure, the EPN, remains unclear. In the present work, we aimed to investigate the role of the EPN in LID and to elucidate the relationship between STN and EPN neuronal activities using single-unit extracellular recordings in urethane anaesthetized 6-OHDA-lesioned rats. In addition, low frequency oscillatory activity and synchronization between the cortex and the EPN were also studied in these parkinsonian rats that received (or not) the chronic treatment with L-DOPA.

2. Materials and methods

2.1. Animals

Male Sprague-Dawley rats (Harlan) weighing 200–250 g at the beginning of the experiments were housed in groups of five in standard laboratory conditions (22 ± 1 °C, 55 ± 5% of relative humidity, and a 12:12 h light/dark cycle) with ad libitum access to food and water. Every effort was made to minimize animal suffering and to use the minimum number of animals per group and experiment. All animal

experiments comply with the ARRIVE guidelines and procedures were approved by the Local Ethical Committee of the University of Basque Country (UPV/EHU), following European (2010/63/EU) and Spanish (RD 53/2013) regulations for the care and use of laboratory animals.

2.2. Drugs

The following drugs were used in this study: isoflurane from Esteve, urethane (1.2 g/kg, i.p.), 6-hydroxydopamine (6-OHDA; 3.5 μg/μl), desipramine hydrochloride (25 mg/kg, i.p.), pargyline (50 mg/kg, i.p.), amphetamine sulphate (3 mg/kg, i.p.), L-DOPA (L-3,4-dihydroxyphenylalanine methyl ester hydrochloride, 6 mg/kg, i.p.) and benserazide-HCL (12 mg/kg, i.p) from Sigma-Aldrich. Desipramine, pargyline, L-DOPA, benserazide and amphetamine sulphate were prepared in 0.9% saline. Urethane was dissolved in MilliQ water. 6-OHDA was dissolved in MilliQ water containing 0.02% ascorbic acid. All drugs were prepared on the day of the experiment.

2.3. Experimental design

The design and timeline of the experiments is shown in Fig. 1A. We characterized the electrophysiological properties of STN and EPN neurons in sham and 6-OHDA-lesioned animals treated chronically either with saline or L-DOPA. Two weeks after surgery (injection of 6-OHDA or vehicle into the medial forebrain bundle (MFB)), the severity of lesion was evaluated with rotational screening and those animals with severe degeneration underwent a 3-week treatment with saline or L-DOPA. During this time, abnormal involuntary movements (AIMs) were scored periodically. All the 6-OHDA-lesioned animals treated with L-DOPA included in these experiments developed dyskinesia and we will refer as long term L-DOPA treated 6-OHDA-lesioned rats. Electrophysiological recordings were obtained 24 h after the last dose of the corresponding treatment (saline or L-DOPA). After STN and EPN baseline recordings were acquired (before L-DOPA), rats received an acute challenge with a standard dose of L-DOPA (6 mg/kg plus benserazide 12 mg/kg, i.p.) and EPN cell recordings were obtained from 20 to 120 min after the drug administration (after L-DOPA). The groups included in this study are referred to as sham saline ($n = 7$), sham L-DOPA ($n = 7$), 6-OHDA saline ($n = 8$) and 6-OHDA L-DOPA (or long term L-DOPA treated 6-OHDA-lesioned) ($n = 9$).

2.4. 6-OHDA lesion and rotational screening

Thirty minutes before the surgery, rats were pre-treated with desipramine (25 mg/kg, i.p.) in order to protect noradrenergic terminals from 6-OHDA toxicity, and with pargyline (50 mg/kg, i.p.) to inhibit monoamine oxidase activity. Rats were deeply anaesthetized with isoflurane (1.5–2%) and 6-OHDA or vehicle was infused (1 μl/min) using a Hamilton. A total of 15.75 μg in 4.5 μl were injected in two sites at right MFB: 2.5 μl at anteroposterior (AP) – 4.4 mm, mediolateral (ML) + 1.2 mm, and dorsoventral (DV) – 7.8 mm, relative to bregma and dura with the toothbar set at −2.4, and 2 μl at AP – 4.0 mm, ML + 0.8 mm, and DV –8 mm, with the toothbar set at +3.4 (Paxinos and Watson, 1997).

The turning behaviour was evaluated 2 weeks post-surgery over 90 min after amphetamine sulphate administration (3 mg/kg, i.p.) as indicator of DA denervation (Miguelez et al., 2011). Severe dopaminergic lesion was represented by > 5 full-body ipsilateral turns/min. Animals were selected for the study and randomly assigned to one of the 6-OHDA groups.

2.5. Abnormal involuntary movement rating

AIMs were induced in 6-OHDA-lesioned rats by chronic daily injections of L-DOPA (6 mg/kg, i.p) in combination with the peripheral decarboxylase inhibitor benserazide (12 mg/kg, i.p.) over 3 weeks. After the chronic treatment was completed, L-DOPA was administered twice per week. AIMs were scored according to a rat dyskinesia scale described by Cenci and Lundblad (2007). Once the scores reached a plateau, L-DOPA dosing was changed to a maintenance (twice a week) schedule (Carlsson et al., 2005). On the testing days, rats were placed individually in transparent empty plastic cages for at least 10 min prior to drug administration. Following L-DOPA injection, each rat was observed for one full minute every 20th min, for a total of 200 min. The frequency of the three subtypes of dyskinetic movements (axial, limb and orolingual AIMs) and asymmetric locomotive behaviour (locomotive AIMs) were rated from 0 to 4, based on the amount of time in which the abnormal movement was present during the observation period (i.e. 0, not present to 4, continuous). In addition, to evaluate the severity of the movements, the amplitude of axial, limb and orolingual AIMs was rated on a scale from 0 to 4. Axial, limb, and orolingual AIMs were analysed separately from locomotive AIMs. Data are expressed as global AIM score/session for axial, limb and orolingual which is calculated multiplying the severity score by the amplitude scores on each monitoring period, with all these products summed for each testing sessions (Lindgren et al., 2010). Locomotive AIMs score/session rates only the frequency of the abnormal movement.

2.6. Electrophysiological procedures

All electrophysiological procedures are schematically illustrated in Fig. 1B. The electrophysiological properties of STN and EPN neurons were investigated after at least 3 weeks of saline or L-DOPA treatment as described in detail by other authors (Jin et al., 2016; Morera-Herreras et al., 2011; Ruskin et al., 2002). Rats were anaesthetized with urethane (1.2 g/kg, i.p.) and placed in a stereotaxic frame with its head secured in a horizontal orientation. Supplementary doses of urethane were administrated during the electrophysiological recordings in order to maintain a proper and constant anaesthesia level, limiting reflexive and reactive responses (Walters et al., 2007). The animal body temperature was maintained at ~37 °C for the entire duration of the experiment by means of a heating pad connected to a rectal probe. The recording electrode, consisting of an Omegadot single glass micropipette with a tip diameter of 1–2.5 μm (approximately 5–7 MΩ) and filled with a 2% solution of Pontamine Sky Blue in 0.5% sodium acetate, was stereotaxically guided to the following coordinates (relative to bregma and dura) ipsilateral to the 6-OHDA injection: for the STN: AP – 3.6 to – 3.8 mm, ML – 2.2 to – 2.7 mm and DV – 7 to – 8 mm; for the EPN AP: – 2.3 to −3 mm, ML: −2.5 mm, DV: −7 to −8.5 mm (Paxinos and Watson, 1997). The extracellular signal from the electrode was amplified with a high-input impedance amplifier, and then monitored on an oscilloscope and on an audio monitor. All recorded STN neurons exhibited a biphasic waveform and a pulse width of 1.0 to 1.5 ms as described by Hollerman and Grace (1992). Recorded EPN neurons showed biphasic waveforms with short wide-duration action potentials 0.8–0.9 ms as described by Ruskin et al. (2002). Neuronal spikes were digitized using computer software (CED micro 1401 interface and Spike2 software, Cambridge Electronic Design, UK). The basal firing rate was recorded for 5–10 min. At the end of experiments, a 5 μA cathodal current was passed through the recording electrode, thus depositing a discrete spot of Pontamine Sky Blue to mark the recording site.

The electrocorticogram (ECoG) was recorded via a 1-mm-diameter steel screw juxtaposed to the dura above the right frontal somatic sensory-motor cortex (AP: +4.5 mm and ML: −2 mm to bregma (Paxinos and Watson, 1997)), as described by Mallet et al. (2008). The signal was pre-amplified (10×), amplified (200×) and bandpass filtered (0.1–1000 Hz) in an amplifier (Cibertec S.A., model amplifier 63 AC). The discriminated ECoG activity (sampled at 2500 Hz) was digitized, stored and analysed using computer software (CED micro 1401 interface and Spike2 software, Cambridge Electronic Design, UK).

The local field potential (LFP) was recorded in the STN and the EPN

(coordinates described above) through the same glass electrodes that were used for single-unit extracellular recordings. The signal was pre-amplified (10×) and then amplified (10×) in a high-input impedance amplifier (Cibertec S.A., model amplifier AE-2) where the signal was also bandpass filtered (0.1–5000 Hz). This signal was divided into two different signals in a second amplifier (Cibertec S.A., model amplifier 63 AC), namely the single-unit extracellular signal and the LFP signal. In this second amplifier, the LFP signal was amplified (10×) and bandpass filtered (0.1–100 Hz). Therefore, single-unit extracellular signals and LFP were recorded at the same time. The discriminated LFP activity (sampled at 2500 Hz) was digitized, stored and analysed using computer software (CED micro 1401 interface and Spike2 software, Cambridge Electronic Design, UK).

It is important to highlight that the ECoG and the LFP were continuously recorded in order to monitor the brain state and to preserve a deep and constant anaesthesia level. This allowed us to avoid modifications in neuronal firing and oscillatory activities related to fluctuations in brain state. This way, our recordings were composed of slow wave activity (SWA), which is characterized by low frequency oscillations. Thus, the results observed in the different groups were obtained in equal conditions and consequently were comparable.

2.7. Histological procedures and analysis

Immediately after the electrophysiological procedure animals were deeply anaesthetized and transcardially perfused with saline followed by 4% ice-cold paraformaldehyde, prepared in 0.1 M phosphate buffer. Brains were removed and transferred to a 25% sucrose solution until they sank. The brains were serially cut in coronal 40 μm sections using a freezing microtome (HM 430, Microm), and slices were conserved in a cryoprotective solution at −20 °C until further processing.

Tyrosine hydroxylase (TH)-immunostaining was used to examine the degree of DA denervation in the striatum and the SNc. Briefly, after endogenous peroxidases inactivation, sections were blocked with 5% normal goat serum, and incubated with rabbit anti-TH (AB 152, 1:1000, Chemicon) primary antibody for 36 h at 4 °C. The sections were then incubated for 2 h with a biotinylated goat antibody against rabbit IgG (BA 1000, 1:200, Vector Laboratories). Thereafter, sections were incubated with an avidin–biotin–peroxidase complex (ABC kit, PK-6100, Vector Laboratories) and peroxidase activity was visualized with 0.05% 3,3′-diaminobenzidine (Sigma) and 0.03% hydrogen peroxide. Finally, sections were mounted onto gelatine-coated slides, dehydrated, cleared with xylene and coverslipped. For the analysis, three striatal sections for each animal (rostral, medial, and caudal levels) were optically digitized and the mean optical density (OD) associated with the striatum was calculated using NIH-produced image analysis software ImageJ (Schneider et al., 2012). The OD was expressed as a percentage of that of the contralateral intact side (100%) with the background associated with the cortex being set as 0%.

For the location of the recording site, brain sections containing the STN or the EPN were mounted on gelatinized glass slides, stained with 1% neutral red, washed, dehydrated, cleared with xylene and coverslipped. Only cells recorded within the STN or EPN have been included in the study.

2.8. Data analysis

The firing parameters of STN and EPN neurons were analysed *off*-line using the Spike2 software. The following parameters were calculated: firing rate and coefficient of variation, which is a measure of firing regularity and is defined as the percentage ratio of the standard deviation to the mean interval histogram. According to the method of Kaneoke and Vitek (1996) and based on the concept of density distribution and on a statistically rigorous definition of the firing pattern, three different firing patterns could be analysed (using the NeuronFit program from NorayBio Informatics): (1) a tonic firing pattern characterized by a symmetrical density distribution histogram, (2) a random firing pattern characterized by a Poisson distribution and (3) a bursting firing pattern characterized by a distribution histogram that is significantly different ($p < .05$) from a Poisson distribution, presenting a significantly positive skew ($p < .05$) of the density distribution histogram and a minimum of four 4 spikes per burst. The analysed spike trains lasted > 120 s and contained at least 300 spikes.

Spike train activity, LFPs and ECoGs were analysed *off*-line by Spike2 software as described in Aristieta et al. (2016). For this purpose, LFP and ECoG signals (sampled at 2500 Hz) were smoothed to 1 ms. Additionally, STN and EPN action potentials were converted to series of events (sampled at 2500 Hz). These series of events were then transformed to a continuous waveform (1-ms smoothing period) (Galati et al., 2009; Galati et al., 2010; Levy et al., 2000), using a custom-made Spike2 software script. Next, cells were classified as oscillatory when the spike waveform autocorrelogram contained a second oscillation peak that was at least twice the magnitude of the random fluctuation (Degos et al., 2005). The power spectrum of smoothed LFPs, ECoGs and STN and EPN spike waveforms were also analysed using the fast Fourier transform (8192 blocks size) in the 0–5 Hz and 0–100 Hz ranges from 90-s epochs of data. The 0 to 100 Hz power spectrum analysis was made to ensure that only low frequency oscillations were presented in the electrophysiological recordings. Coherence analyses between EPN spike waveforms and LFPs; EPN spike waveforms and ECoGs; STN spike waveforms and LFPs; and STN spike waveforms and ECoGs were performed using the fast Fourier transform function of Spike2 software (8192 block size). The mean coherence was calculated for the 0–5 Hz range from 90-s epochs of data. The significance of the coherence was determined by the equation described by Rosenberg et al. (1989): $1 - (1 - \alpha)\ 1 / (L - 1)$, where α is 0.95 and L is the number of windows used. The area under the curve (AUC) of coherence and power spectrum curves were calculated in the 0 to 5 Hz frequency range, in all groups. To study the phase relationship between ECoGs/EPN spikes; LFPs/EPN spikes; ECoGs/STN spikes; and LFPs/STN spikes, spike-triggered waveform averages (STWAs) were performed from smoothed ECoG or LFP recordings and EPN or STN spikes from 90-s epochs of data. The amplitudes of the peak to trough values at or around zero time were compared in the different groups of rats. Spikes occurring in the peak and trough were considered to be at 0° and 180° phase, respectively (Parr-Brownlie et al., 2007). Additionally, the phase-locking relationship of ECoG recordings, STN spike and EPN spike trains was also analysed. ECoG signals were band-pass filtered at 0–5 Hz (Spike2). This way, peaks in the ECoG correspond to a phase of 0° and the troughs to a phase of 180°. Phase histograms were constructed in Spike2 (Mallet et al., 2008) and the modulation of each neuron firing activity in relationship with cortical low frequency oscillations was analysed using the Rayleigh's test (MATLAB). The null hypothesis for Rayleigh's test is that the spikes are distributed in a uniform manner. The mean phase angle and the mean resultant vector length (vector length) were calculated for each neuron and circular plots were created as described by Sharott et al. (2017). The vector length of the phase distribution was used to analyze the phase locking level around the mean phase for individual neurons, calculated quantifying the angle of every single spike. Then, it was also calculated for populations of neurons, using the mean angle of each neuron. The vector length of the phase distribution was measured from 0 to 1, where values closer to 1 corresponded to more concentrated spike angles, and therefore lower variance in the distribution around the mean phase angle of each neuron (i.e. higher level of phase locking). In the circular plots, the vector lengths of the mean phases of firing of single neurons were expressed as lines radiating from the center, while each dot indicated the mean phase angle of every individual neuron. Finally, the mean vector length (VL) value and the mean phase angle (PA) value were calculated for each specific population of neurons.

2.9. Statistical analysis of data

Experimental data were analysed using the computer programme GraphPad Prism (v. 5.01, GraphPad Software, Inc). TH OD in the striatum was analysed using paired Student's *t*-test (lesioned versus unlesioned side). The electrophysiological data were analysed by two way analysis of variance ANOVA (lesion × treatment) followed by post hoc comparisons using the Bonferroni post hoc test. The effect of the acute L-DOPA challenge on the synchronization and oscillatory activity was analysed using unpaired Student's *t*-test (before versus after L-DOPA). The firing pattern of STN and EPN neurons was analysed using Fisher's exact test. Simple linear regression analyses were used to assess correlations between different data. The level of statistical significance was set at $p < .05$. Data are presented as the group mean ± standard error of the mean (S.E.M.). Detailed information regarding statistical results is shown in the Supplementary Table S3.

3. Results

3.1. Development of L-DOPA-induced abnormal involuntary movements

As showed in previous publications (Aristieta et al., 2012; Aristieta et al., 2016; Azkona et al., 2014; Cenci et al., 1998; Miguelez et al., 2011), the chronic L-DOPA administration (6 mg/kg plus benserazide 12 mg/kg, i.p.) resulted in a rapid induction of dyskinesia in 6-OHDA-lesioned rats. During the first week of treatment, the severity of axial, limb and orolingual AIMs increased before reaching a plateau by the second week (Supplementary Fig. 1). We did not detect any AIMs in the rest of the groups, including sham saline, sham L-DOPA and 6-OHDA saline rats. The evaluation of the time course of the AIMs after a single injection of L-DOPA showed the expected profile with the first signs appearing 10–20 min after the drug injection, reaching a peak between 40 and 80 min and subsiding by 180–200 min (Supplementary Fig. 1). The extent of the nigral lesion and striatal DA denervation was confirmed later by TH immunohistochemistry. All animals with the 6-OHDA lesion included in the study showed >95% reduction in TH-fibre density in the striatum on the side ipsilateral to the lesion.

3.2. Increased irregular and bursting firing activity in the entopeduncular nucleus of long term L-DOPA treated 6-OHDA-lesioned rats

A total of 214 GABAergic neurons were recorded in the EPN 24 h after the last saline or L-DOPA injection (baseline): 41 neurons from the sham saline group ($n = 7$ animals), 45 neurons from the sham L-DOPA group ($n = 7$ animals), 56 neurons from the 6-OHDA saline group ($n = 8$ animals) and 72 neurons from the 6-OHDA L-DOPA group ($n = 9$ animals). All the cells recorded displayed the characteristic firing patterns of GABAergic EPN neurons, narrow spike waveform, and were localized within the EPN. The results showed no significant differences in the firing rate among groups (Fig. 2A and Table S3). However, we found that the coefficient of variation was increased in the 6-OHDA L-DOPA group compared to the rest of the groups ($p < .001$) (Table 1, Table S3 and Fig. 2B). The analysis of the firing pattern revealed that the number of bursting pattern neurons was increased in both 6-OHDA-lesioned groups when compared to sham animals ($p < .001$) (Fig. 2C). After recording basal activity, 160 neurons were also recorded between 20 and 120 min after an acute challenge of L-DOPA, which is the time period corresponding with intense dyskinetic behaviour (Fig. 2A, B and C): 34 neurons from the sham saline group ($n = 7$ animals), 31 neurons from the sham L-DOPA group ($n = 7$ animals), 37 neurons from the 6-OHDA saline group ($n = 8$ animals) and 58 neurons from the 6-OHDA L-DOPA group ($n = 9$ animals). The acute challenge of L-DOPA only produced an effect on the L-DOPA-treated groups (Table S3). Thus, the increased coefficient of variation and bursting firing pattern observed in the 6-OHDA L-DOPA group were partially reversed ($p < .001$ and $p < .01$, respectively, unpaired Student's *t*-test and $p < .05$, Fisher's exact test), while the coefficient of variation was also significantly reduced after the acute challenge in sham L-DOPA group ($p < .05$ unpaired Student's *t*-test) (Fig. 2B and C). When the behavioural and electrophysiological parameters of long term L-DOPA treated 6-OHDA-lesioned rats were analysed together, there was no statistically significant correlation between the electrophysiological properties of EPN neurons and the measured AIMs (Tables S1 and S2).

3.3. Correlation between subthalamic nucleus and entopeduncular nucleus neuron activity in long term L-DOPA treated 6-OHDA-lesioned rats

In order to evaluate the relationship between the STN and the EPN firing parameters, STN glutamatergic neurons were recorded before performing EPN recordings in the same rats from the four experimental groups: 52 neurons from the sham saline group ($n = 7$ animals), 62 neurons from the sham L-DOPA group ($n = 7$ animals), 80 neurons from the 6-OHDA saline group ($n = 8$ animals) and 88 neurons from the 6-OHDA L-DOPA group ($n = 9$ animals). As we previously showed, there were significant differences between the sham and 6-OHDA-lesioned groups in the basal electrophysiological parameters of STN neurons (Table 1 and Table S3), which corresponded to the hyperactive STN state that is typical of DA denervated condition (Aristieta et al., 2012; Aristieta et al., 2016). Next, we analysed the relationship between STN and EPN firing parameter mean values (firing rate, coefficient of variation and firing pattern) that were obtained in the same rats. We did not find any correlation between the mean firing rate of STN and EPN neurons, which were recorded 24 h after the last injection of saline or L-DOPA (Fig. 2D). However, we found that there was a significant correlation for the coefficient of variation in the 6-OHDA L-DOPA group ($p < .05$) (Fig. 2E). Similarly, in these long term L-DOPA treated 6-OHDA-lesioned rats, there was a significant correlation between the proportion of bursting STN and EPN neurons ($p < .05$) (Fig. 2F). The rest of the groups did not show any correlation for the coefficient of variation and the firing pattern (data not shown).

3.4. The acute L-DOPA challenge reversed the increased low frequency oscillatory activity and synchronization in the entopeduncular nucleus in long term L-DOPA treated 6-OHDA-lesioned rats

In all the experimental groups (sham saline, sham L-DOPA, 6-OHDA saline and 6-OHDA L-DOPA), EPN neurons showing a non-bursting (regular) firing pattern did not exhibit any kind of synchronization with the simultaneously recorded EPN-LFPs and/or ECoGs (Fig. 3A, left). Moreover, the spike wave autocorrelograms of these neurons showed no oscillatory activity (Fig. 3B, left). In contrast, EPN neurons expressing a bursting firing pattern showed an oscillatory activity as observed in the autocorrelogram analysis (Fig. 3A and B, right). This oscillatory activity was coupled to the simultaneously recorded EPN-LFPs and ECoGs (Fig. 3A, right). The EPN spikes within the bursts were correlated with the troughs of the EPN-LFPs and with the peak of the ECoGs. As described in Fig. 3C, the proportion of neurons that showed oscillatory activity was significantly higher in 6-OHDA-lesioned groups than in non-lesioned groups ($p < .05$, Fisher's exact test), and the chronic L-DOPA treatment did not induce any change. However, the acute L-DOPA challenge in long term L-DOPA treated 6-OHDA-lesioned rats significantly reduced the proportion of EPN neurons showing oscillatory pattern (from 58% to 42%; $p < .05$, Fisher's exact test), as previously observed for the bursting pattern.

Twenty-four hours after the last dose of L-DOPA (or saline), the power spectra analysis in the 0–5 Hz frequency range for the ECoG and the EPN-LFP showed a similar peak in all the experimental groups with a mean frequency of 0.5–1 Hz and similar AUC values (Fig. 4A and D and Table S3). Nevertheless, in the 6-OHDA L-DOPA group the AUC value of the EPN-LFP was significantly higher than in the sham groups ($p < .05$) (Fig. 4F). The acute L-DOPA challenge only increased

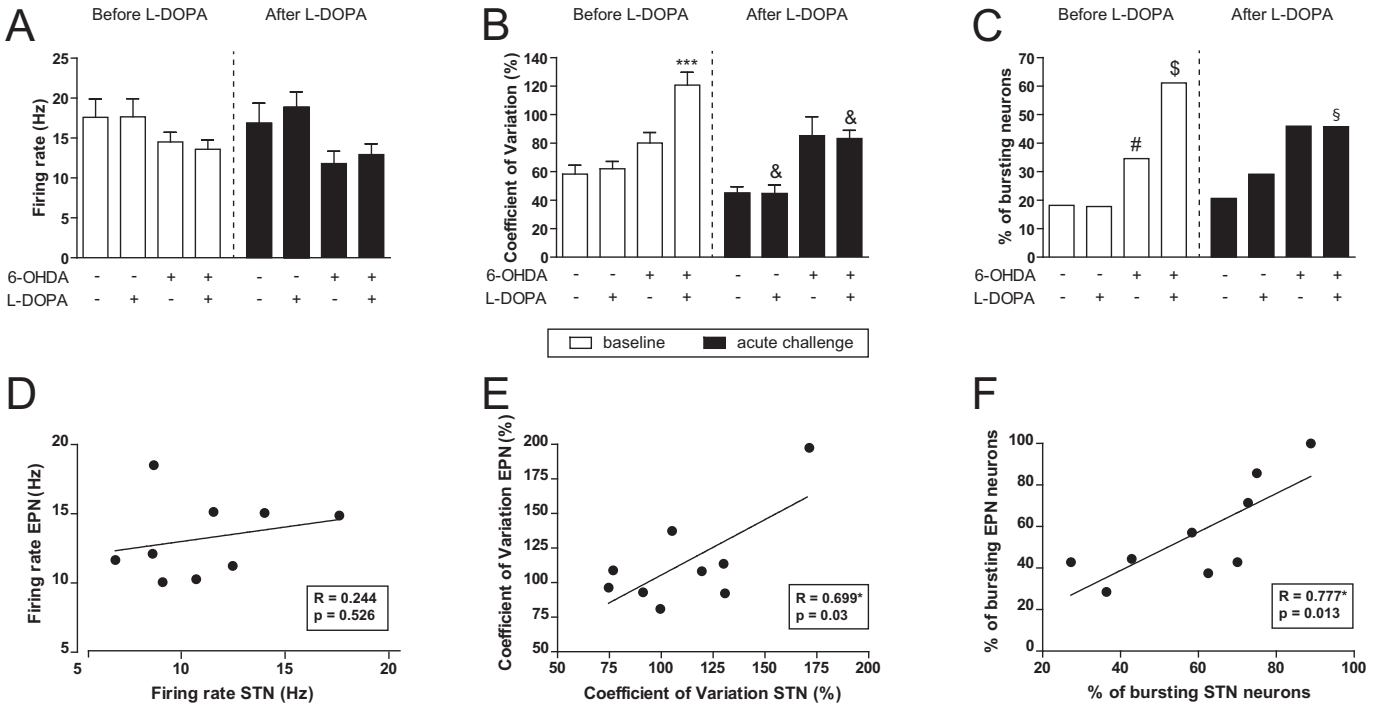

Fig. 2. Electrophysiological characterization of the Entopeduncular nucleus, and regression analysis between STN neurons and EPN neurons electrophysiological parameters recorded in the same rat. ***(A)*** Firing rate (Hz) of EPN GABAergic neurons. Baseline firing rate (white bars) was not significantly different in the four experimental groups. The acute challenge of L-DOPA (6 mg/kg, i.p.) plus benserazide (12 mg/kg i.p.) (black bars) did not modify the firing rate in the different experimental groups. ***(B)*** Coefficient of variation (%). Baseline activity (white bars) was significantly increased in 6-OHDA L-DOPA group. The acute challenge of L-DOPA plus benserazide produced a significant reduction in sham L-DOPA and 6-OHDA L-DOPA groups. ***(C)*** Firing pattern of EPN cells expressed as percentage of neurons. Baseline bursting firing pattern (white bars) was significantly increased in 6-OHDA lesioned groups. After the acute challenge of L-DOPA plus benserazide, the number of bursting neurons was reduced in the 6-OHDA L-DOPA group. ***(D)*** Pearson r value for the correlation between the firing rate of STN neurons and EPN neurons recorded 24 h after the last L-DOPA injection in the same long term L-DOPA treated 6-OHDA-lesioned rats. ***(E)*** Pearson r value for the correlation between the coefficient of variation of STN neurons and EPN neurons recorded 24 h after the last L-DOPA injection in the same long term L-DOPA treated 6-OHDA-lesioned rats. ***(F)*** Pearson r value for the correlation between the percentage of bursting neurons of STN neurons and EPN neurons recorded 24 h after the last L-DOPA injection in the same long term L-DOPA treated 6-OHDA-lesioned rats. Data are expressed as mean ± S.E.M. *** $p < .001$ vs. sham saline and sham L-DOPA (Bonferroni's *post-hoc* test); $^{\&}$ $p < .05$ vs. its baseline (unpaired *t*-test). $^{\#}$ $p < .05$ vs. sham L-DOPA (Fisher's exact-test for firing pattern); $ $p < .05$ vs. sham saline, sham L-DOPA and 6-OHDA saline (Fisher's exact-test for firing pattern); § $p < .05$ vs. its baseline (Fisher's exact-test for firing pattern); * $p < .05$ (Pearson r value).

significantly the AUC value of the ECoG power spectrum curve in the 6-OHDA L-DOPA group ($p < .05$, unpaired Student's *t*-test) (Fig. 4B and C). The acute L-DOPA challenge also increased the AUC values of the EPN-LFP power spectrum curves in sham saline ($p < .05$, unpaired Student's *t*-test) and sham L-DOPA ($p < .001$, unpaired Student's *t*-test) groups (Fig. 4F), while, the AUC value of the EPN-LFP power spectrum curve was reduced ($p < .01$, unpaired Student's *t*-test) in the 6-OHDA L-DOPA group (Fig. 4E and F). Note that non remarkable oscillatory activity was found in other oscillatory frequency bands (Supplementary Fig. 4C, D, E and F).

In basal conditions (before L-DOPA), coherence analysis between simultaneously recorded EPN spike trains (transformed to continuous waveforms) and ECoGs showed that the coherence peak appeared in a similar frequency value (approximately 1 Hz) without differences among the experimental groups (Fig. 5A). Nevertheless, the AUC values extracted from the coherence curves were significantly higher in 6-OHDA-lesioned groups compared to non-lesioned groups, and were not modified by the chronic L-DOPA treatment (Fig. 5A and C and Table S3). However, the acute L-DOPA challenge increased the coherence AUC value in sham L-DOPA rats ($p < .01$, unpaired Student's *t*-test), while, the AUC value in the 6-OHDA L-DOPA group was reduced ($p < .01$, unpaired Student's *t*-test) (Fig. 5B and C). Similarly, the

Table 1
Basal electrophysiological properties of EPN and STN neurons recorded 24 h after the last saline or L-DOPA administration. The firing pattern is presented as percentage of neurons which represent the standard discharge patterns of EPN and STN neurons.* $p < .05$, ** $p < .01$ and *** $p < .001$ vs. sham saline and sham L-DOPA (Bonferroni's *post-hoc* test), $^{\$}$ $p < .001$ vs. the rest of the groups (Bonferroni's *post-hoc* test), $^{\#}$ $p < .05$ and $^{\#\#}$ $p < .001$ vs. sham saline and sham L-DOPA.

Groups	EPN					STN				
	Firing rate (Hz)	Coefficient of variation (%)	Firing pattern			Firing rate (Hz)	Coefficient of Variation (%)	Firing pattern		
			Tonic	Random	Bursting			Tonic	Random	Bursting
Sham saline	17,60 ± 2,29	58,30 ± 6,20	70.46	11.37	18.18	6,25 ± 0,56	72,46 ± 3,93	53,74	14,92	31,34
Sham L-DOPA	17,66 ± 2,26	62,03 ± 5,16	75.55	6.67	17.78	6,84 ± 0,71	71,45 ± 4,39	56,45	14,51	29,04
6-OHDA saline	14,51 ± 1,22	80,04 ± 7,37	$56.36^{\#\#}$	9.09	$34.55^{\#\#}$	9,98 ± 0,88*	115,6 ± 6,15***	$43,18^{\#}$	7,95	$48,87^{\#}$
6-OHDA L-DOPA	13,60 ± 1,17	120,7 ± 8,93***	$31.94^{\$}$	6.95	$61.11^{\$}$	10,96 ± 0,86**	112,0 ± 6,36***	$41,75^{\#\#}$	6,59	$51,65^{\#\#}$

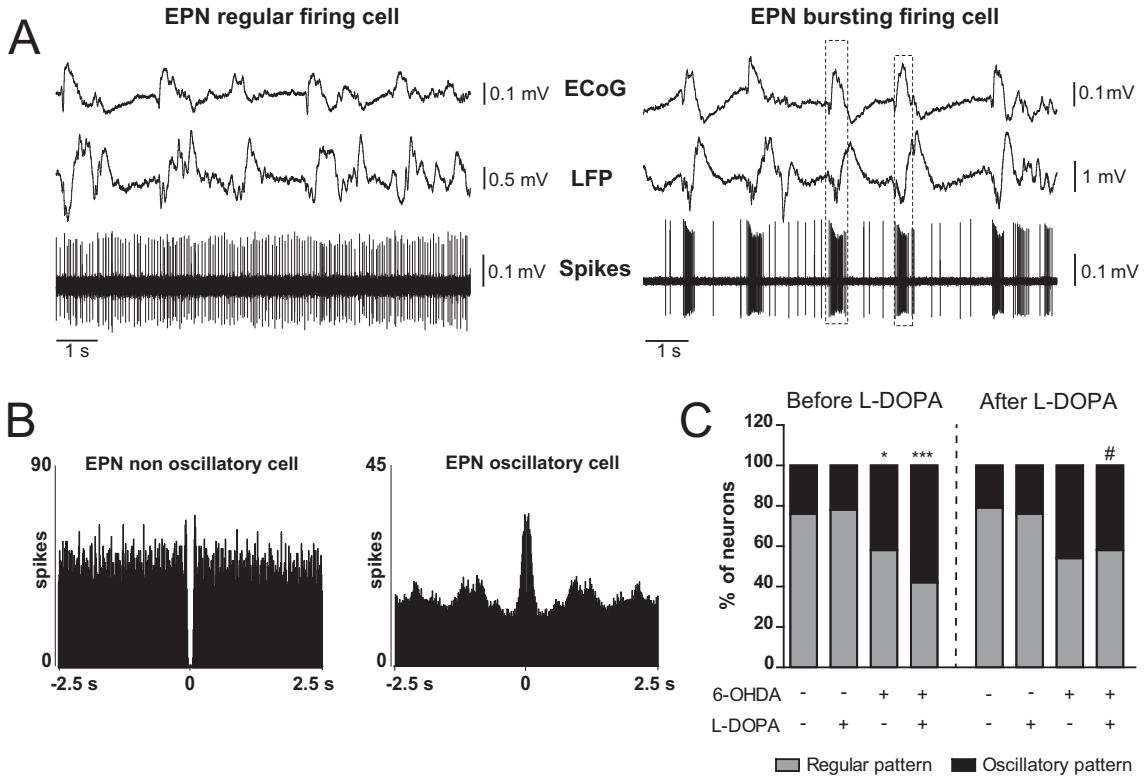

Fig. 3. Effect of 6-OHDA lesion and L-DOPA treatment on the oscillatory activity of the EPN and the ECoG. ***(A)*** A recording track containing EPN spikes, EPN-LFP and ECoG from a neuron which exhibited a regular firing pattern (left), the most common neuron firing pattern in sham saline and sham L-DOPA groups. A recording track containing EPN spikes, EPN-LFP and ECoG from a neuron which exhibited a bursting firing pattern (right), the most representative neuron firing pattern in 6-OHDA saline and 6-OHDA L-DOPA groups. ***(B)*** On the left, autocorrelograms showing the pattern of a non-oscillatory EPN neuron (left) and the pattern of an oscillatory EPN neuron (right). ***(C)*** Oscillatory pattern of EPN neurons expressed as percentage of neurons. The oscillatory activity of EPN neurons was significantly higher in 6-OHDA lesioned groups. While the acute L-DOPA challenge reduced the proportion of oscillatory EPN neurons in 6-OHDA L-DOPA group. $^{*}p < .05$ and $^{***}p < .001$ for both groups vs. their respective controls (Fisher's exact-test); $^{\#}p < .05$ vs. its baseline (Fisher's exact test).

coherence analysis of simultaneously recorded EPN spike trains (transformed to continuous waveforms) and EPN-LFPs also showed that coherence peak values appeared near 1 Hz in the four experimental groups (Fig. 5D). The AUC values obtained from the coherence between EPN spikes and EPN-LFP curves were significantly higher in 6-OHDA-lesioned groups than in non-lesioned groups (Fig. 5D and E and Table S3). The acute L-DOPA challenge reduced the coherence AUC value in long term L-DOPA treated 6-OHDA-lesioned rats ($p < .01$, unpaired Student's *t*-test) (Fig. 5E and F).

The analysis of the STWAs revealed that EPN neurons tended to discharge near the peak of the ECoG recordings in all the experimental groups (Fig. 6A). The peak to trough amplitude of ECoG/ EPN spikes STWAs was significantly higher in the 6-OHDA L-DOPA group compared to sham groups ($p < .01$) (Fig. 6A and C and Table S3), and it was reduced by the acute L-DOPA challenge ($p < .001$, unpaired Student's *t*-test) (Fig. 6B and C). In addition, EPN neurons tended to discharge near the trough of the EPN-LFP recordings in all the experimental groups (Fig. 6D). The analysis of the EPN-LFP/ EPN spikes STWAs showed that the peak to trough amplitude was significantly higher in the 6-OHDA L-DOPA group compared to non-lesioned groups ($p < .01$) (Fig. 6D and F and Table S3). The acute L-DOPA challenge reduced the peak to trough amplitude in these long term L-DOPA treated 6-OHDA-lesioned rats ($p < .001$, unpaired Student's *t*-test) (Fig. 6E and F).

3.5. Increased low frequency oscillatory activity in the subthalamic nucleus after the 6-OHDA lesion

As we previously described (Aristieta et al., 2016), the 6-OHDA lesion increased the proportion of STN neurons that showed bursting firing pattern (Table 1). The activity of these neurons was coupled to simultaneously recorded STN-LFPs and ECoGs. The STN spikes were correlated with the troughs of the STN-LFP and the peaks of the ECoG (Supplementary Fig. 2A). Indeed, autocorrelogram analysis showed increased oscillatory activity in STN neurons after the 6-OHDA lesion, while the L-DOPA treatment did not induce any modification (Supplementary Fig. 2B).

Additionally, the power spectra analysis in the 0–5 Hz frequency range, showed a peak with a mean frequency of 0.5–1.5 Hz in all the experimental groups. In the ECoG power spectrum there were no differences among the groups (Supplementary Fig. 2C left and Table S3). Nevertheless, the analysis of the STN-LFP power spectrum showed that the 6-OHDA lesion increased the AUC values, while the L-DOPA treatment did not produce any change (Supplementary Fig. 2C right and Table S3). Note that non remarkable oscillatory activity was found in other oscillatory frequency bands (Supplementary Fig. 4A and B).

Coherence analysis between simultaneously recorded STN spikes (transformed to continuous waveforms) and ECoGs or STN-LFPs (0–5 Hz frequency range), showed a similar coherence peak in the different groups (approximately 1 Hz) (Supplementary Fig. 3A and B, respectively). However, AUC values obtained from coherence curves were significantly higher in 6-OHDA-lesioned groups compared to non-lesioned groups (Supplementary Fig. 3A and B top, respectively and Table S3). This increased coherence observed in 6-OHDA-lesioned groups was not altered after chronic L-DOPA treatment (Supplementary Fig. 3A and B top, respectively).

The STWA analysis showed that STN spikes tended to discharge near the trough of the STN-LFP recordings in all the experimental

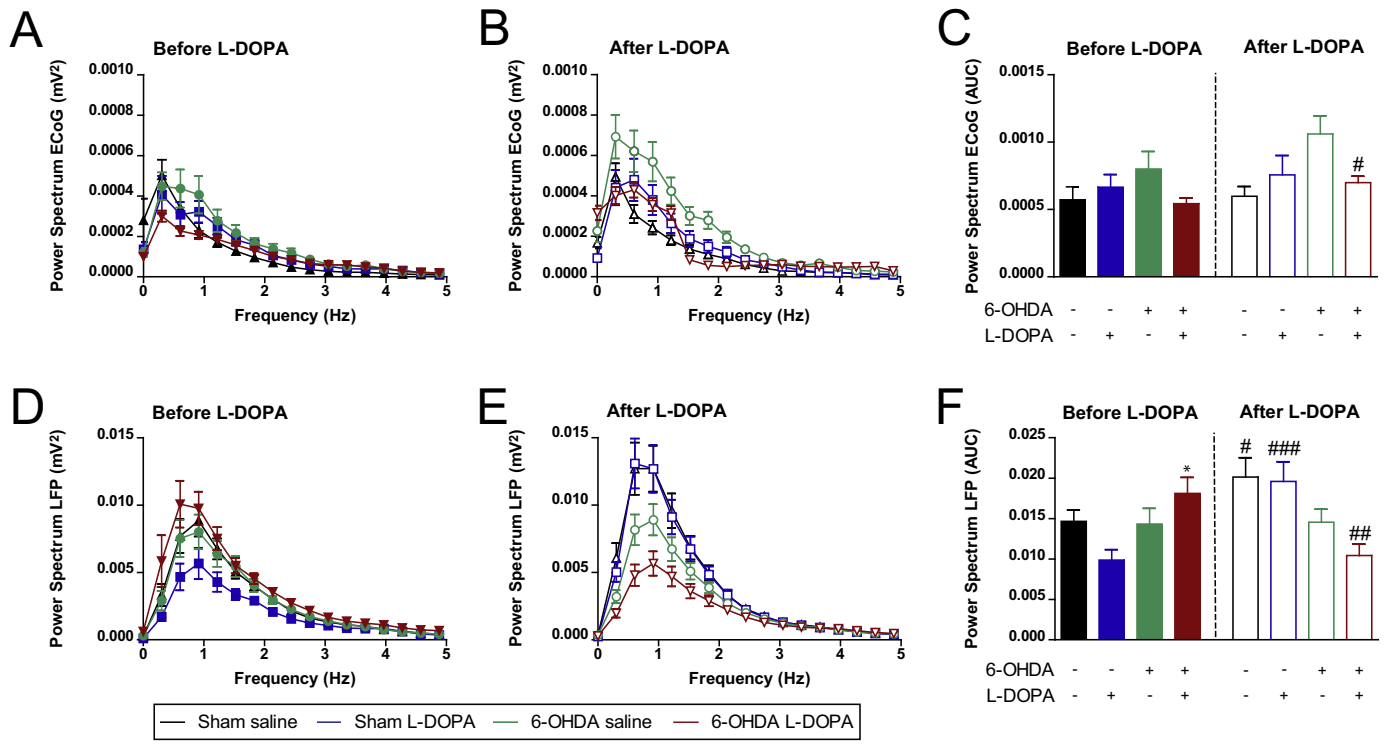

Fig. 4. Effect of 6-OHDA lesion and L-DOPA treatment on the power spectrum of the EPN-LFP and the ECoG. Area under the curve (AUC) values obtained from power spectrum curves (0–5 Hz frequency range) were used to analyze the power spectrum of the ECoG ***(A, B and C)*** and EPN-LFP ***(D, E and F)*** in the different groups ***(A)*** ECoG power spectrum analysis, in the 0–5 Hz frequency range, in sham saline, sham L-DOPA, 6-OHDA saline and 6-OHDA L-DOPA groups 24 h after the last L-DOPA or saline injection. Not significant differences were found among the groups ***(A)***. After the acute L-DOPA challenge the AUC value was increased in the power spectrum of the 6-OHDA L-DOPA group ***(B and C)***. ***(D)*** EPN-LFP power spectrum analysis, in the 0–5 Hz frequency range, in sham saline, sham L-DOPA, 6-OHDA saline and 6-OHDA L-DOPA groups 24 h after the last L-DOPA or saline injection. The 6-OHDA L-DOPA groups showed increased LFP power spectrums compared to sham saline and sham L-DOPA groups ***(D)***. After the acute L-DOPA challenge the AUC values were increased in sham saline and sham L-DOPA groups ***(E and F)***, while it was reduced in 6-OHDA L-DOPA group ***(E and F)***. Data are expressed as mean ± S.E.M. * $p < .05$ vs. sham saline and sham L-DOPA (Bonferroni's *post-hoc* test); $^{\#}p < .05$; $^{\#\#}p < .01$ and $^{\#\#\#}p < .001$ vs. its baseline (unpaired t-test).

groups (Supplementary Fig. 3D). The analysis of the peak to trough amplitude of STN-LFP/STN spike STWAs revealed that 6-OHDA lesion increased this amplitude, and the L-DOPA treatment did not produce any modification (Supplementary Fig. 3D top and Table S3). In contrast, STN neurons tended to discharge near the peak of the ECoG recordings, in all groups (Supplementary Fig. 3C). The peak to trough analysis of ECoG/STN spikes STWAs did not reveal any significant difference among the groups (Supplementary Fig. 3C top and Table S3).

3.6. The L-DOPA challenge reduced the proportion of phase-locked entopeduncular nucleus neurons in long term L-DOPA treated 6-OHDA-lesioned rats

Finally, the phase relationship of the ECoG, STN spike and EPN spike trains was also analysed. The ECoG recordings were filtered at 0–5 Hz and the phase analysis was developed as described before (see materials and methods). Only neurons showing significant phase-locking determined by Rayleigh's test were included for phase angle and vector length analysis. STN and EPN neurons spike trains presented a phase relationship, showing tendency to discharge more in the ascending face of the filtered ECoG (0–5 Hz) in the 6-OHDA-lesioned groups (Fig. 7A and B). The proportion of STN neurons presenting a significant phase-locked relationship in time with low frequency oscillatory activity (recorded 24 h after the last L-DOPA or saline injection) was increased in 6-OHDA-lesioned groups compared to their control groups (24/60 vs 45/77, sham saline and 6-OHDA saline respectively, $p < .05$, Fisher's exact test; 21/53 vs 55/81 sham L-DOPA and 6-OHDA L-DOPA respectively, $p < .01$, Fisher's exact test) (Fig. 7A and B upper panels). Nevertheless, in the EPN only long term L-DOPA treated 6-OHDA-lesioned rats (recorded 24 h after the last L-DOPA injection) showed augmented proportion of phase-locked spike trains (10/44 vs 43/72, sham L-DOPA and 6-OHDA L-DOPA respectively, $p < .001$, Fisher's exact test) (Fig. 7B middle panels). In this group of rats, the acute L-DOPA challenge reduced this augmented proportion of phase-locked EPN spike trains ($p < .01$, Fisher's exact test) (Fig. 7B bottom panels). No significant differences in the mean phase angle were found among the different experimental groups for STN spike and EPN spike trains (Fig. 7A and B and Table S3). Similarly, we did not observe any significant difference in the vector length for STN spike and EPN spike trains in the different groups (Fig. 7A and B and Table S3).

4. Discussion

The present work extends our previous results regarding the BG output nucleus, SNr (Aristieta et al., 2016), obtained in the well-characterized hemiparkinsonian and dyskinetic rat model (Cenci et al., 1998; Winkler et al., 2002). Here, new results concerning the other BG output structure show that the nigrostriatal degeneration plus the L-DOPA treatment induces alterations in the activity of EPN neurons that correlate with STN hyperactivity. This modified EPN activity observed in long term L-DOPA treated 6-OHDA-lesioned rats together with the increment in low frequency oscillatory activity and synchronization is partially reversed by the acute L-DOPA administration. Altogether, these results suggest that the prolonged L-DOPA treatment in 6-OHDA-lesioned rats induces changes in the EPN closely related to the STN hyperactivity. Moreover, the reversion of the altered firing pattern, low frequency oscillatory activity and synchronization observed within the EPN in the 6-OHDA L-DOPA group (after acute L-DOPA challenge) seem

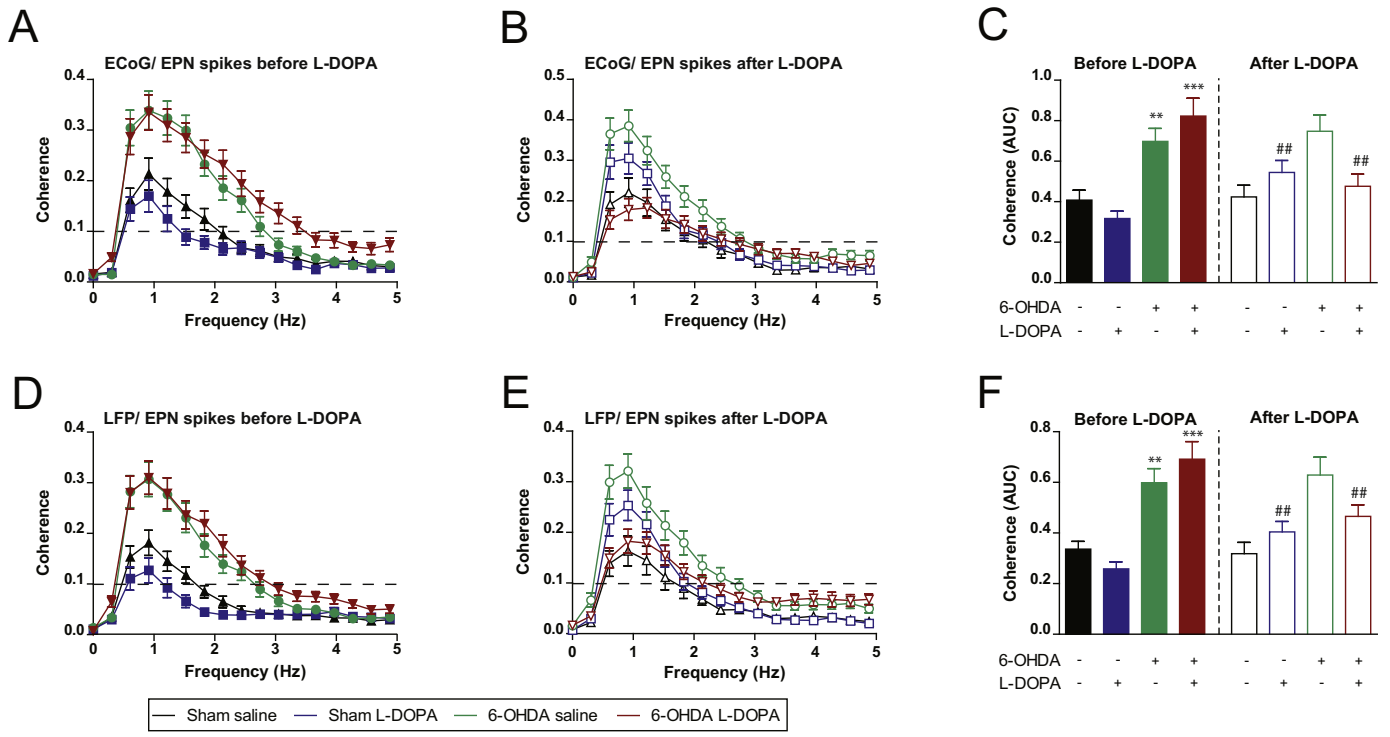

Fig. 5. Effect of 6-OHDA lesion and L-DOPA treatment on EPN spike trains, EPN-LFP and ECoG coherence. ***(A and C)*** Coherence power between the ECoG and EPN spikes (converted into a continuous waveform) simultaneously recorded in sham saline, sham L-DOPA, 6-OHDA saline and 6-OHDA L-DOPA groups, in the 0–5 Hz frequency range. Area under the curve values obtained from coherence curves were used to analyze the ECoG/ EPN spikes coherence, in the 0–5 Hz frequency range. The coherence between the ECoG and EPN spikes was increased in 6-OHDAsaline and 6-OHDA L-DOPA groups compared to sham saline and sham L-DOPA groups respectively. ***(B and C)*** The acute L-DOPA challenge increased the coherence between the ECoG and EPN spikes in sham L-DOPA group. Nevertheless, the coherence between the ECoG and EPN spikes in 6-OHDA L-DOPA was reduced after the acute L-DOPA challenge. ***(D and F)*** Coherence power between the EPN-LFP and EPN spikes (converted into a continuous waveform) simultaneously recorded in the different experimental groups, in the 0–5 Hz frequency range. Area under the curve values obtained from coherence curves were used to analyze the EPN-LFP/ EPN spikes coherence, in the 0–5 Hz frequency range. The coherence between the EPN-LFP and EPN spikes was augmented in 6-OHDA saline and 6-OHDA L-DOPA groups compared to their respective control groups. ***(E and F)*** The acute L-DOPA challenge reduced the coherence between the EPN-LFP and EPN spike in 6-OHDA L-DOPA group. Data are expressed as mean ± S.E.M. In ***(A)***, ***(B)***, ***(D)*** and ***(E)*** the horizontal dashed line indicates $p = .05$. ** $p < .01$ vs. sham saline and *** $p < .001$ vs. sham L-DOPA (Bonferroni's *post-hoc* test); $^{\#\#}$ $p < .01$ vs its baseline (unpaired *t* test).

to be related to the LID.

4.1. EPN activity and abnormal involuntary movements

In this study, we found that the DA denervation modified the firing pattern of EPN neurons, increasing the number of bursting neurons as previously shown in 6-OHDA-lesioned rats (Ruskin et al., 2002) and 1-methyl-4-phenyl, 1,2,3,6-tetrahydropyridine (MPTP) treated monkeys (Boraud et al., 1998). The classical BG model (Alexander et al., 1986) predicts that after the DA loss, the firing activity of the EPN should be increased. However, results in agreement and disagreement with this model have been extensively published. Results obtained from metabolic markers analysis in 6-OHDA lesioned rats (Lacombe et al., 2009; Périer et al., 2003) and electrophysiological recordings in MPTP treated monkeys (Boraud et al., 1998) support the BG model predictions. In contrast, results obtained from EPN neuron recordings in rats have revealed no changes in the firing rate of EPN neurons after 6-OHDA lesion (Ruskin et al., 2002). Our results are in line with these last findings suggesting that in rodents the consequences of the nigrostriatal lesion are associated with alterations in the firing pattern rather than a simple increase in the firing rate of the BG output nuclei. This fact may induce an increase of neurotransmitter levels in the projection areas of the EPN since neurons which exhibit bursting firing pattern release more neurotransmitter than neurons with regular firing pattern (Chergui et al., 1996; Florin-lechner et al., 1996).

Some authors link the development of LID with a decreased firing rate and metabolic activity of the GPi/EPN (Lacombe et al., 2009; Papa et al., 1999). Thus, L-DOPA injections reduce the firing rate of EPN or GPi neurons below control values in 6-OHDA-lesioned rats (Jin et al., 2016) and MPTP treated monkeys (Boraud et al., 1998; Papa et al., 1999) as well as the metabolic activity of the EPN in 6-OHDA lesioned rats (Lacombe et al., 2009; Périer et al., 2003). In the same line, in our hands, the acute L-DOPA challenge partially reversed the increment in firing irregularity and in the number of bursting neurons induced by prolonged L-DOPA treatment in the EPN of 6-OHDA-lesioned animals. These results suggest that the EPN may have a direct role in the motor symptomatology associated with LID, although we did not observe any correlation between EPN neuron activity and the scored AIMs in 6-OHDA-lesioned rats treated with L-DOPA.

4.2. STN activity and correlation with EPN activity

The STN is the sole glutamatergic nucleus in the BG and it's strategically located in the hyperdirect and indirect pathways, converging the information coming from these two different pathways. In this study we found that the DA denervation increased STN activity as previously shown by us and others (Aristieta et al., 2012, 2016; Bergman et al., 1994; Hassani et al., 1996; Magill et al., 2001; Morera-Herreras et al., 2011; Vila et al., 2000). Thus, STN neuron firing rate, coefficient of variation and the proportion of neurons that exhibited bursting firing pattern increased after the 6-OHDA lesion. In addition, the L-DOPA chronic treatment did not modify the STN hyperactivity, as we have

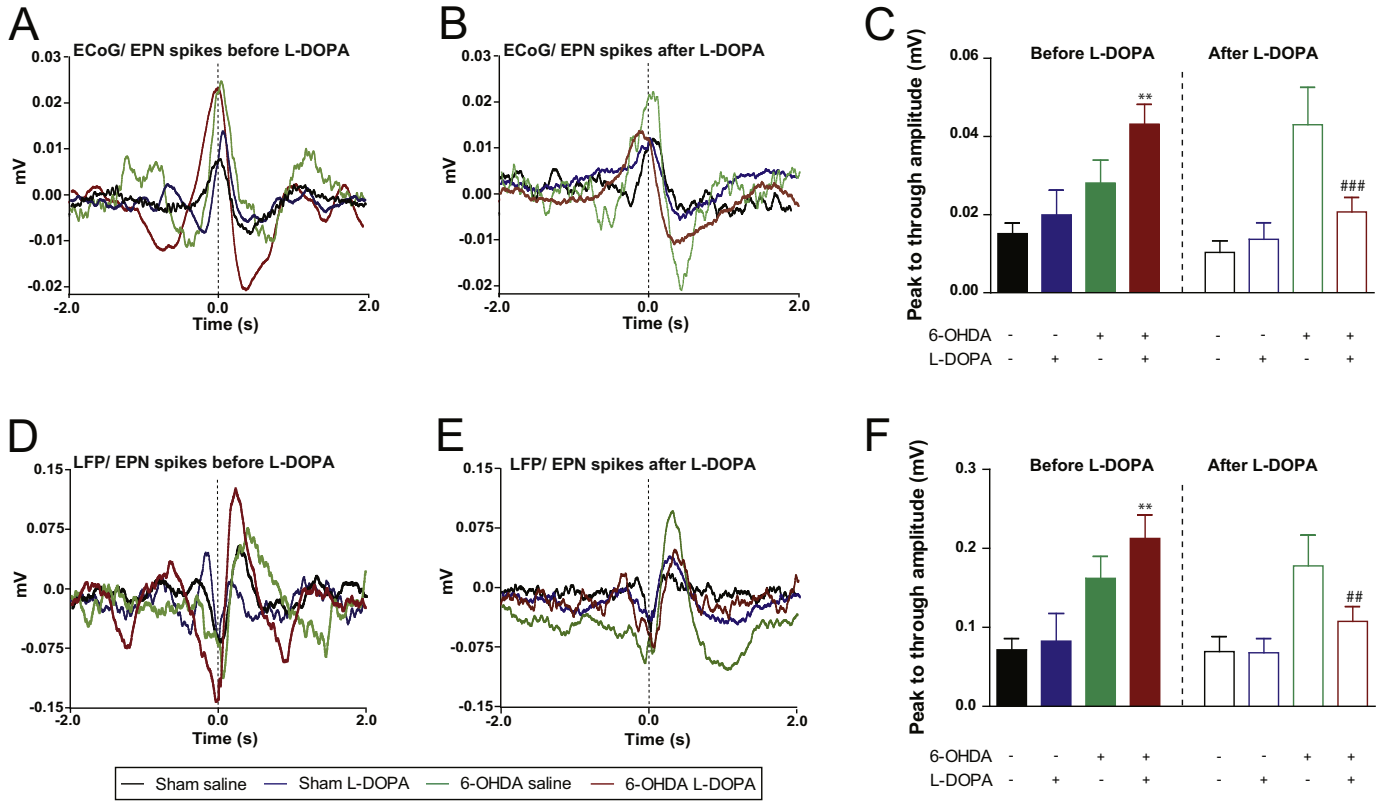

Fig. 6. Effect of 6-OHDA lesion and L-DOPA treatment on the spike triggered waveform averages. ***(A and C)*** Spike triggered waveform averages (STWAs) illustrating the relationship between the ECoG and EPN spikes ***(A)*** and the EPN-LFP and EPN spikes ***(D)*** simultaneously recorded in sham saline, sham L-DOPA, 6-OHDA saline and 6-OHDA L-DOPA groups. The analysis of STWAs was made measuring the peak to trough amplitudes in the different groups of rats. ***(A and C)*** The peak to trough amplitude value of ECoG/ EPN spikes STWA was significantly higher in 6-OHDA L-DOPA group compared to sham saline and sham L-DOPA groups. ***(B and C)*** The acute L-DOPA challenge reduced the peak to trough amplitude value of ECoG/ EPN spikes STWA in 6-OHDA L-DOPA group. ***(C and F)*** In EPN-LFP/ EPN spikes the peak to trough amplitude values of the STWA was increased in the 6-OHDA L-DOPA group compared to sham saline and sham L-DOPA groups. ***(E and F)*** The acute L-DOPA challenge reduced the peak to trough amplitude value of EPN-LFP/ EPN spikes STWA in the 6-OHDA L-DOPA group. Data are expressed as mean ± S.E.M. ** $p < .01$ vs. sham saline and sham L-DOPA (Bonferroni's *post-hoc* test); $^{\#\#}$ $p < .01$ and $^{\#\#\#}$ $p < .001$ vs. its baseline (unpaired *t* test).

previously observed (Aristieta et al., 2012, 2016). These findings could be explained by the desensitization of the DA receptors that modulate STN activity (Bouthenet et al., 1987; Boyson et al., 1986; Flores et al., 1999; Johnson et al., 1994). Alternatively, the lack of effect of L-DOPA on STN activity may be due to the loss of SN input (Brown et al., 1979; Canteras et al., 1990; Mitchell et al., 1989) after 6-OHDA lesion which may reduce L-DOPA conversion into DA. Indeed, microiontophoretic administration of DA exerts a direct action on STN neurons (Ni et al., 2001).

We observed two positive correlations, one between STN and EPN baseline coefficient of variation values and another one between the proportion of bursting firing pattern neurons recorded in the STN and the EPN from 6-OHDA-lesioned rats chronically treated with L-DOPA. We did not find any other correlation in the rest of experimental groups. Previously we have found a correlation between the firing rate of SNr and the STN neurons (Aristieta et al., 2016). Altogether these results suggest that L-DOPA chronic treatment after DA degeneration induced changes that increase the driving force of the STN on the BG output structures.

4.3. EPN neuron oscillatory activity and synchronization

To the best of our knowledge, this is the first time that low frequency oscillatory activity (0–5 Hz) and synchronization has been deeply studied in the EPN from parkinsonian and dyskinetic animals.

Using 6-OHDA lesioned animals, several studies have revealed the expression of SWA of approximately 1 Hz frequency in the rat cortex, GP, STN and SNr and an increased cortical/BG synchronization at this low frequency after the lesion (or tetrodotoxin administration) in urethane anaesthetized rats (Aristieta et al., 2016; Galati et al., 2009, 2010; Magill et al., 2001; Parr-Brownlie et al., 2007; Walters et al., 2007). In the same line, we also found SWA (1 Hz frequency approximately) and an increased proportion of neurons showing low frequency oscillatory activity in the EPN after the 6-OHDA lesion. Others have reported, however, a reduction of neurons presenting low frequency oscillatory activity after the 6-OHDA injection (Ruskin et al., 2002). As described for the other BG output structure, we did not find changes in the power spectra of EPN-LFP and ECoG (Aristieta et al., 2016; Belluscio et al., 2003; Meissner et al., 2006). The coherence analysis indicated that the peak of synchronization between EPN spikes and EPN-LFP or ECoG was at 1 Hz approximately, and that EPN neuron discharge happened near the peak of the ECoG and the trough of the LFP, similar to the SNr (Aristieta et al., 2016; Belluscio et al., 2003; Galati et al., 2010; Meissner et al., 2006). Coherence between EPN neuronal activity and EPN-LFP or ECoG was enhanced following 6-OHDA lesion, corroborating that the DA denervation augmented the synchronization between these neuronal populations. However, the STWA analysis did not show a significant increase of the synchronization between EPN spiking activity and EPN-LFP or ECoG after the 6-OHDA lesion. The peak to trough amplitude was not significantly larger in the 6-OHDA-lesioned group although there was a tendency.

The chronic L-DOPA treatment did not modify the augmented coherence between the ECoG and the EPN spikes or the EPN-LFP and the EPN spikes (0–5 Hz frequency range) observed in 6-OHDA-lesioned rats but increased the synchronization between those areas. As STWA analysis showed, synchronization between EPN spiking activity and EPN-

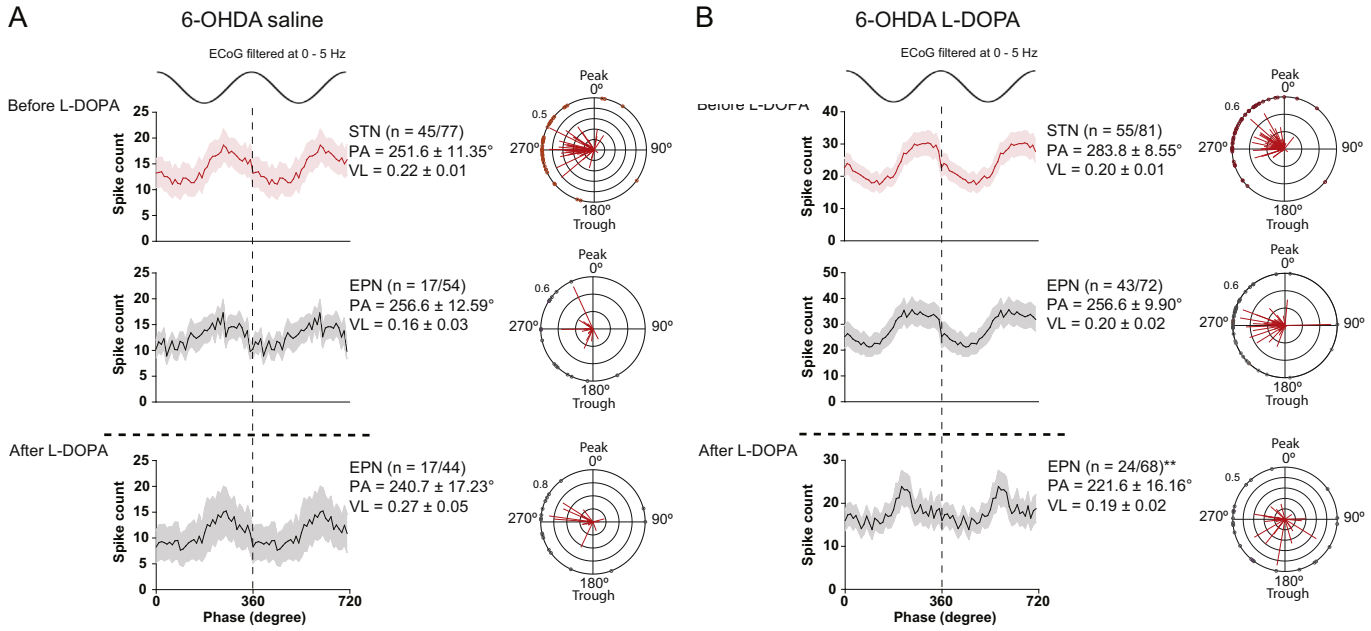

Fig. 7. Phase relationship of STN and EPN neurons in 6-OHDA saline and 6-OHDA L-DOPA rats during low frequency oscillatory activity. ***(A and B)*** Linear phase histograms of the firing rate and circular plots showing the firing angles of significantly phase locked STN and EPN neurons in 6-OHDA saline ***(A)*** and 6-OHDA L-DOPA ***(B)*** rats during low frequency oscillations (0–5 Hz). Two cycles of low frequency oscillations were represented for better clarification. In the circular plots, the vector lengths of the mean phases of firing of single neurons were expressed as lines radiating from the center (the vector length indicates the variance in the distribution of spikes around the mean phase angle of each neuron), while each dot indicated the mean phase angle of every individual neuron. STN and EPN neurons showed a phase relationship with preference to fire in the ascending phase of the low frequency oscillations in 6-OHDA saline ***(A)*** and 6-OHDA L-DOPA ***(B)*** rats. Notice that after the 6-OHDA lesion the proportion of significantly phase locked STN neurons was increased ***(A and B upper)***. However, in the EPN the proportion of significantly phase locked neurons was only increased in 6-OHDA L-DOPA rats ***(B middle)***. In this group, the acute L-DOPA challenge significantly reduced the proportion of significantly phase locked EPN neurons ***(B down)***. PA represented the mean phase angle (in degree) of a specific population of neurons. VL represented the mean vector length of a specific population of neurons. Data are expressed as mean ± S.E.M. $^{**}p < .01$ vs. its baseline (Fisher's exact test).

LFP or ECoG was higher because the peak to trough amplitude was larger in the 6-OHDA L-DOPA group. In this group of animals, the power spectrum value of EPN-LFP was also increased in the low frequency band (0–5 Hz). Moreover, the proportion of EPN neurons showing phase-locked relationship in time with low frequency oscillations was increased after the L-DOPA treatment in 6-OHDA-lesioned rats. This supports the idea that the chronic L-DOPA treatment augmented even more the increased low frequency oscillatory activity observed in the EPN in 6-OHDA-lesioned rats. On the other hand, the acute L-DOPA challenge reversed the increased low frequency oscillatory activity and synchronization observed in the 6-OHDA L-DOPA group. Indeed, the power spectrum value of EPN-LFP was reduced in the low frequency band (0–5 Hz) after the acute L-DOPA challenge in these long term L-DOPA treated 6-OHDA-lesioned rats. In addition, the coherence between EPN neuronal activity and EPN-LFP or ECoG was also reduced after the acute L-DOPA challenge in the 6-OHDA L-DOPA group. Moreover, the STWA analysis also demonstrated that the synchronization between EPN spiking activity and EPN-LFP or ECoG was reversed after the acute L-DOPA challenge in long term L-DOPA treated 6-OHDA-lesioned rats. The STWA peak to trough amplitude was smaller in this group as well as the proportion of phase-locked EPN neurons. Other groups have also reported similar results in other oscillatory frequency ranges. Jin et al. (2016) found that 6-OHDA lesioned animals had increased coherence between EPN spikes and motor cortex ECoG in theta and beta frequency bands. In this case, the L-DOPA challenge reduced these theta and beta oscillatory activities and synchronization in dyskinetic rats, but also beta coherence in 6-OHDA drug-naïve animals. Our recording protocol was similar to the one used by Jin et al. (2016), however, we did not observed significant theta and beta oscillatory activities probably because all our experiments were performed in a very deep anaesthesia state, and the parameters used for the analysis were not exactly the same. Indeed, our ECoG recordings were composed of strong SWA, which is mainly characterized by low frequency oscillatory activity (Galati et al., 2009, 2010; Magill et al., 2001). Electrophysiological recordings performed in urethane anesthetized rats have demonstrated that this anaesthesia evokes different brain states (Jin et al., 2016; Mallet et al., 2008) that fluctuate from large amplitude slow waves to an “activated state” as a consequence of spontaneous variations or external sensory stimuli (Jin et al., 2016; Magill et al., 2006; Mallet et al., 2008). In 6-OHDA lesioned rats, the transition from the SWA to the “activated state” can induce the appearance of beta oscillatory activity (Alam et al., 2012; Jin et al., 2016; Mallet et al., 2008; Sharott et al., 2005). In some of these works the transition was evoked by hindpaw pinching (Mallet et al., 2008; Sharott et al., 2005), while other authors showed this transition spontaneously (Alam et al., 2012; Jin et al., 2016; Rumpel et al., 2013). Note that beta band oscillatory activity is only present during the “activated state”, and not during SWA (Alam et al., 2012; Rumpel et al., 2013), and no transition to cortical activation state was found in our ECoG recordings. In addition, it is worth mentioning that deep brain stimulation of the EPN reduces LID in 6-OHDA-lesioned rats. This effect on LID is accompanied by several modifications in oscillatory activity at different frequency ranges (theta, beta and gamma) in the striatum (Alam et al., 2014).

4.4. STN neuron oscillatory activity and synchronization

As previously described and discussed by us and others (Aristieta et al., 2016; Magill et al., 2001; Parr-Brownlie et al., 2007; Walters et al., 2007), the 6-OHDA lesion increased the low frequency oscillatory activity and synchronization in the STN and between this nucleus and the motor cortex. Moreover, the L-DOPA treatment did not induce remarkable modifications in the low frequency oscillatory activity in the STN.

Interestingly, our recordings demonstrated that STN and EPN neurons showed a phase firing relationship to ongoing low frequency oscillatory activity during SWA. STN and EPN neurons presented a tendency to discharge more in the ascending face of the ECoG, both in sham and 6-OHDA-lesioned groups. However, the incidence of this phase-locked activity was higher after DA depletion in the STN, while in the EPN was only more pronounced in the 6-OHDA L-DOPA group. These results also support the idea that alterations of low frequency oscillatory activity and synchronization in the STN emerged from DA degeneration. Nevertheless, in the EPN, this modified low oscillatory activity was only remarkable in the 6-OHDA L-DOPA group, where the acute L-DOPA challenge reduced the proportion of phase-locked neurons. All these results suggest that LID may be related to reversed low frequency oscillatory activity and synchronization in the EPN.

5. Conclusion

Cortical information is transmitted to the STN and the EPN through several BG pathways. Thus, the increased oscillatory activity and synchronization observed following the DA degeneration may be consequence of complex interactions between different circuits. Indeed, increased abnormal rhythms have been associated with PD symptoms (Quiroga-Varela et al., 2013), although a deeper understanding of the pathophysiology of PD is necessary to improve its treatment (Ellens and Leventhal, 2013). Clinical studies have shown that the reduction on dyskinesia induced by deep brain stimulation on the GPi is superior to that induced by stimulation on the STN (see review Ramirez-Zamora and Ostrem, 2018). Our previous results have shown a modest role of the STN in LID in 6-OHDA-lesioned rats (Aristieta et al., 2012). The present work shows that, in rats after the denervation of the nigrostriatal DA pathway long term treatment of L-DOPA increases the interaction between the STN and the EPN. Probably as consequence of changes that include modifications in firing pattern and spiking phase. However, our results, in line with the mentioned clinical studies, suggest that what it seems relevant in LID is the reversion of changes in the low frequency oscillatory activity, the proportion of phase-locked neurons and the synchronization within the EPN and between this nucleus and the cortex. In summary, the EPN may be a good target to treat LID since the degeneration of nigral DA neurons combined with L-DOPA treatment induces some changes in it that when they are reversed lead to the appearance of dyskinesia.

Supplementary data to this article can be found online at https://doi.org/10.1016/j.expneurol.2019.113036.

Acknowledgements

Supported by: the Spanish Government, MINECO, SAF2016-77758-R (AEI/FEDER, UE) and the Government of the Basque Country T747-13. We would like to thank UPV/EHU SGIker for their collaboration as for the animal housing. A.A had a fellowship from the University of the Basque Country.

Declarations of interest

None.

References

Ahlskog, J.E., Muenter, M.D., 2001. Frequency of levodopa-related dyskinesias and motor fluctuations as estimated from the cumulative literature. Mov. Disord. 16, 448–458. https://doi.org/10.1002/mds.1090.

Alam, M., Heissler, H.E., Schwabe, K., Krauss, J.K., 2012. Deep brain stimulation of the pedunculopontine tegmental nucleus modulates neuronal hyperactivity and enhanced beta oscillatory activity of the subthalamic nucleus in the rat 6-hydroxydopamine model. Exp. Neurol. 233, 233–242. https://doi.org/10.1016/j.expneurol.2011.10.006.

Alam, M., Capelle, H.H., Schwabe, K., Krauss, J.K., 2014. Effect of deep brain stimulation on levodopa-induced dyskinesias and striatal oscillatory local field potentials in a rat model of Parkinson's disease. Brain Stimul. 7 (1), 13–20. https://doi.org/10.1016/j.brs.2013.09.001.

Alexander, G.E., DeLong, M.R., Strick, P.L., 1986. Parallel organization of functionally segregated circuits linking basal ganglia and cortex. Annu. Rev. Neurosci. 9, 357–381. https://doi.org/10.1146/annurev.neuro.9.1.357.

Alonso-Frech, F., Zamarbide, I., Alegre, M., Rodríguez-Oroz, M.C., Guridi, J., Manrique, M., Valencia, M., Artieda, J., Obeso, J.A., 2006. Slow oscillatory activity and levodopa-induced dyskinesias in Parkinson's disease. Brain 129, 1748–1757. https://doi.org/10.1093/brain/awl103.

Aristieta, A., Azkona, G., Sagarduy, A., Miguelez, C., Ruiz-Ortega, J.Á., Sanchez-Pernaute, R., Ugedo, L., 2012. The role of the subthalamic nucleus in L-DOPA induced dyskinesia in 6-hydroxydopamine lesioned rats. PLoS One 7. https://doi.org/10.1371/journal.pone.0042652.

Aristieta, A., Ruiz-Ortega, J.A., Miguelez, C., Morera-Herreras, T., Ugedo, L., 2016. Chronic L-DOPA administration increases the firing rate but does not reverse enhanced slow frequency oscillatory activity and synchronization in substantia nigra pars reticulata neurons from 6-hydroxydopamine-lesioned rats. Neurobiol. Dis. 89, 88–100. https://doi.org/10.1016/j.nbd.2016.02.003.

Azkona, G., Sagarduy, A., Aristieta, A., Vazquez, N., Zubillaga, V., Ruiz-Ortega, J.A., Perez-Navarro, E., Ugedo, L., Sanchez-Pernaute, R., 2014. Buspirone anti-dyskinetic effect is correlated with temporal normalization of dysregulated striatal DRD1 signalling in l-DOPA-treated rats. Neuropharmacology 79, 726–737. https://doi.org/10.1016/j.neuropharm.2013.11.024.

Belluscio, M.A., Kasanetz, F., Riquelme, L.A., Murer, M.G., 2003. Spreading of slow cortical rhythms to the basal ganglia output nuclei in rats with nigrostriatal lesions. Eur. J. Neurosci. 17, 1046–1052. https://doi.org/10.1046/j.1460-9568.2003.02543.x.

Bergman, H., Wichmann, T., Karmon, B., DeLong, M.R., 1994. The primate subthalamic nucleus. II. Neuronal activity in the MPTP model of parkinsonism. J. Neurophysiol. 72, 507–520.

Boraud, T., Bezard, E., Guehl, D., Bioulac, B., Gross, C., 1998. Effects of L-DOPA on neuronal activity of the globus pallidus externalis (GPe) and globus pallidus internalis (GPi) in the MPTP-treated monkey. Brain Res. 787, 157–160. https://doi.org/10.1016/S0006-8993(97)01563-1.

Bouthenet, M.L., Martres, M.P., Sales, N., Schwartz, J.C., 1987. A detailed mapping of dopamine D-2 receptors in rat central nervous system by autoradiography with [125I]iodosulpride. Neuroscience 20, 117–155. https://doi.org/10.1016/0306-4522(87)90008-X.

Boyson, S.J., McGonigle, P., Molinoff, P.B., 1986. Quantitative autoradiographic localization of the D1 and D2 subtypes of dopamine receptors in rat brain. J. Neurosci. 6, 3177–3188.

Brown, L.L., Markman, M.H., Wolfson, L.I., Dvorkin, B., Warner, C., Katzman, R., 1979. A direct role of dopamine in the rat subthalamic nucleus and an adjacent intrapeduncular area. Science 206, 1416–1418. https://doi.org/10.1126/science.505015. 80-.

Canteras, N.S., Shammah-Lagnado, S.J., Silva, B.A., Ricardo, J.A., 1990. Afferent connections of the subthalamic nucleus: a combined retrograde and anterograde horseradish peroxidase study in the rat. Brain Res. 513, 43–59. https://doi.org/10.1016/0006-8993(90)91087-W.

Carlsson, T., Winkler, C., Burger, C., Muzyczka, N., Mandel, R.J., Cenci, A., Björklund, A., Kirik, D., 2005. Reversal of dyskinesias in an animal model of Parkinson's disease by continuous L-DOPA delivery using rAAV vectors. Brain 128, 559–569. https://doi.org/10.1093/brain/awh374.

Cenci, M.A., Lee, C.S., Björklund, A., 1998. L-DOPA-induced dyskinesia in the rat is associated with striatal overexpression of prodynorphin- and glutamic acid decarboxylase mRNA. Eur. J. Neurosci. 10, 2694–2706. https://doi.org/10.1046/j.1460-9568.1998.00285.x.

Cenci, M.A., Lundblad, M., 2007. Ratings of L-DOPA-induced dyskinesia in the unilateral 6-OHDA lesion model of Parkinson's disease in rats and mice. Curr Protoc Neurosci. https://doi.org/10.1002/0471142301.ns0925s41. Chapter 9:Unit 9.25.

Chergui, K., Nomikos, G.G., Mathé, J.M., Gonon, F., Svensson, T.H., 1996. Burst stimulation of the medial forebrain bundle selectively increases Fos-like immunoreactivity in the limbic forebrain of the rat. Neuroscience 72, 141–156. https://doi.org/10.1016/0306-4522(95)00513-7.

Degos, B., Deniau, J., Thierry, A., Glowinski, J., Pezard, L., 2005. Neuroleptic-induced catalepsy: electrophysiological mechanisms of functional recovery induced by high-frequency stimulation of the subthalamic nucleus. J. Neurosci. 25, 7687–7696. https://doi.org/10.1523/JNEUROSCI.1056-05.2005.

Ellens, D.J., Leventhal, D.K., 2013. Electrophysiology of basal ganglia and cortex in models of parkinson disease. J. Park. Dis. 3, 241–254. https://doi.org/10.3233/JPD-130204.

Flores, G., Liang, J.J., Sierra, A., Martinez-Fong, D., Quirion, R., Aceves, J., Srivastava, L.K., 1999. Expression of dopamine receptors in the subthalamic nucleus of the rat: characterization using reverse transcriptase-polymerase chain reaction and autoradiography. Neuroscience 91, 549–556. https://doi.org/10.1016/S0306-4522(98)00633-2.

Florin-lechner, S.M., Druhan, J.P., Aston-Jones, G., Valentino, R.J., 1996. Enhanced norepinephrine release in prefrontal cortex with burst stimulation of the locus coeruleus. Brain Res. 742 (1–2), 89–97.

Fogelson, N., Williams, D., Tijssen, M., van Bruggen, G., Speelman, H., Brown, P., 2006. Different functional loops between cerebral cortex and the subthalmic area in Parkinson's disease. Cereb. Cortex 16, 64–75. https://doi.org/10.1093/cercor/bhi084.

Galati, S., Stanzione, P., D'Angelo, V., Fedele, E., Marzetti, F., Sancesario, G., Procopio, T., Stefani, A., 2009. The pharmacological blockade of medial forebrain bundle induces an acute pathological synchronization of the cortico-subthalamic nucleus-globus

pallidus pathway. J. Physiol. 587, 4405–4423. https://doi.org/10.1113/jphysiol.2009.172759.
Galati, S., D'Angelo, V., Olivola, E., Marzetti, F., Di Giovanni, G., Stanzione, P., Stefani, A., 2010. Acute inactivation of the medial forebrain bundle imposes oscillations in the SNr: a challenge for the 6-OHDA model? Exp. Neurol. 225, 294–301. https://doi.org/10.1016/j.expneurol.2010.06.020.
Giannicola, G., Rosa, M., Marceglia, S., Scelzo, E., Rossi, L., Servello, D., Menghetti, C., Pacchetti, C., Zangaglia, R., Locatelli, M., Caputo, E., Cogiamanian, F., Ardolino, G., Barbieri, S., Priori, A., 2013. The effects of levodopa and deep brain stimulation on subthalamic local field low-frequency oscillations in Parkinson's disease. Neurosignals 21, 89–98. https://doi.org/10.1159/000336543.
Hammond, C., Bergman, H., Brown, P., 2007. Pathological synchronization in Parkinson's disease: networks, models and treatments. Trends Neurosci. 30 (7), 357–364. https://doi.org/10.1016/j.tins.2007.05.004.
Hassani, O.K., Mouroux, M., Feger, J., 1996. Increased subthalamic neuronal activity after nigral dopaminergic lesion independent of disinhibition via the globus pallidus. Neuroscience 72, 105–115.
Hollerman, J.R., Grace, A.A., 1992. Subthalamic nucleus cell firing in the 6-OHDA-treated rat: basal activity and response to haloperidol. Brain Res 590, 291–299.
Horak, F.B., Anderson, M.E., 1984. Influence of globus pallidus on arm movements in monkeys. II. Effects of stimulation. J. Neurophysiol. 52, 305–322. https://doi.org/10.1152/jn.1984.52.2.305.
Jin, X., Schwabe, K., Krauss, J.K., Alam, M., 2016. Coherence of neuronal firing of the entopeduncular nucleus with motor cortex oscillatory activity in the 6-OHDA rat model of Parkinson's disease with levodopa-induced dyskinesias. Exp. Brain Res. 234, 1105–1118. https://doi.org/10.1007/s00221-015-4532-1.
Johnson, A.E., Coirini, H., Kallstrom, L., Wiesel, F.-A., 1994. Characterization of dopamine receptor binding sites in the subthalamic nucleus. Neuroreport 5, 1836–1838.
Kaneoke, Y., Vitek, J.L., 1996. Burst and oscillation as disparate neuronal properties. J. Neurosci. Methods 68, 211–223. https://doi.org/10.1016/0165-0270(96)00081-7.
Kühn, A.A., Kupsch, A., Schneider, G., Brown, P., 2006. Reduction in subthalamic 8–35 °Hz oscillatory activity correlates with clinical improvement in Parkinson's disease. Eur. J. Neurosci. 23, 1956–1960. https://doi.org/10.1111/j.1460-9568.2006.04717.x.
Lacombe, E., Khaindrava, V., Melon, C., Oueslati, A., Kerkerian-Le Goff, L., Salin, P., 2009. Different functional basal ganglia subcircuits associated with anti-akinetic and dyskinesiogenic effects of antiparkinsonian therapies. Neurobiol. Dis. 36, 116–125. https://doi.org/10.1016/j.nbd.2009.07.002.
Levy, R., Hutchison, W.D., Lozano, a M., Dostrovsky, J.O., 2000. High-frequency synchronization of neuronal activity in the subthalamic nucleus of parkinsonian patients with limb tremor. J. Neurosci. 20, 7766–7775 doi:20/20/7766 [pii].
Lindgren, H.S., Andersson, D.R., Lagerkvist, S., Nissbrandt, H., Cenci, M.A., 2010. L-DOPA-induced dopamine efflux in the striatum and the substantia nigra in a rat model of Parkinson's disease: temporal and quantitative relationship to the expression of dyskinesia. J. Neurochem. 112, 1465–1476. https://doi.org/10.1111/j.1471-4159.2009.06556.x.
Lozano, A.M., Lang, A.E., Levy, R., Hutchison, W., Dostrovsky, J., 2000. Neuronal recordings in Parkinson's disease patients with dyskinesias induced by apomorphine. Ann. Neurol. 47, S141–S146.
Magill, P.J., Bolam, J.P., Bevan, M.D., 2001. Dopamine regulates the impact of the cerebral cortex on the subthalamic nucleus-globus pallidus network. Neuroscience 106, 313–330. https://doi.org/10.1016/S0306-4522(01)00281-0.
Magill, P.J., Pogosyan, A., Sharott, A., Csicsvari, J., Bolam, J.P., Brown, P., 2006. Changes in functional connectivity within the rat striatopallidal axis during global brain activation in vivo. J. Neurosci. 26, 6318–6329. https://doi.org/10.1523/JNEUROSCI.0620-06.2006.
Mallet, N., Pogosyan, A., Sharott, A., Csicsvari, J., Bolam, J.P., Brown, P., Magill, P.J., 2008. Disrupted dopamine transmission and the emergence of exaggerated beta oscillations in subthalamic nucleus and cerebral cortex. J. Neurosci. 28, 4795–4806. https://doi.org/10.1523/JNEUROSCI.0123-08.2008.
Meissner, W., Ravenscroft, P., Reese, R., Harnack, D., Morgenstern, R., Kupsch, A., Klitgaard, H., Bioulac, B., Gross, C.E., Bezard, E., Boraud, T., 2006. Increased slow oscillatory activity in substantia nigra pars reticulata triggers abnormal involuntary movements in the 6-OHDA-lesioned rat in the presence of excessive extracelullar striatal dopamine. Neurobiol. Dis. 22, 586–598. https://doi.org/10.1016/j.nbd.2006.01.009.
Miguelez, C., Aristieta, A., Cenci, M.A., Ugedo, L., 2011. The locus coeruleus is directly implicated in l-Dopa-Induced dyskinesia in parkinsonian rats: An electrophysiological and behavioural study. PLoS One 6. https://doi.org/10.1371/journal.pone.0024679.
Mink, J., 1996. The basal ganglia: focused selection and inhibition of competing motor programs. Prog. Neurobiol. 50, 381–425. https://doi.org/10.1016/S0301-0082(96)00042-1.
Mitchell, I.J., Clarke, C.E., Boyce, S., Robertson, R.G., Peggs, D., Sambrook, M.A., Crossman, A.R., 1989. Neural mechanisms underlying parkinsonism symptoms based upon regional brain uptake of 2-deoxyglucose in monkeys exposed to N-methyl-4-phenyl-1,2,3,6-tetrahydropyridine. Neuroscience 32, 213–226.
Morera-Herreras, T., Ruiz-Ortega, J.Á., Linazasoro, G., Ugedo, L., 2011. Nigrostriatal denervation changes the effect of cannabinoids on subthalamic neuronal activity in rats. Psychopharmacology 214, 379–389. https://doi.org/10.1007/s00213-010-2043-0.
Ni, Z., Gao, D., Bouali-Benazzouz, R., Benabid, A.L., Benazzouz, A., 2001. Effect of microiontophoretic application of dopamine on subthalamic nucleus neuronal activity in normal rats and in rats with unilateral lesion of the nigrostriatal pathway. Eur. J. Neurosci. 14, 373–381. https://doi.org/10.1046/j.0953-816X.2001.01644.x.
Obeso, J.A., Rodriguez-Oroz, M.C., Rodriguez, M., DeLong, M.R., Olanow, C.W., 2000. Pathophysiology of levodopa-induced dyskinesias in Parkinson's disease: problems with the current model. Ann. Neurol. 47, S22–S32 discussion S32–4.
Olanow, C.W., Brin, M.F., Obeso, J.A., 2000. The role of deep brain stimulation as a surgical treatment for Parkinson's disease. Neurology 55, S60–S66.
Papa, S.M., Desimone, R., Fiorani, M., Oldfield, E.H., 1999. Internal globus pallidus discharge is nearly suppressed during levodopa- induced dyskinesias. Ann. Neurol. 46, 732–738. https://doi.org/10.1002/1531-8249(199911)46:5<732::AID-ANA8>3.0.CO;2-Q.
Parr-Brownlie, L.C., Poloskey, S.L., Flanagan, K.K., Eisenhofer, G., Bergstrom, D.A., Walters, J.R., 2007. Dopamine lesion-induced changes in subthalamic nucleus activity are not associated with alterations in firing rate or pattern in layer V neurons of the anterior cingulate cortex in anesthetized rats. Eur. J. Neurosci. 26, 1925–1939. https://doi.org/10.1111/j.1460-9568.2007.05814.x.
Paxinos, G., Watson, C., 1997. The Rat Brain in Stereotaxic Coordinates, third ed. Academic Press, Orlando.
Périer, C., Marin, C., Jimenez, A., Bonastre, M., Tolosa, E., Hirsch, E.C., 2003. Effect of subthalamic nucleus or entopeduncular nucleus lesion on levodopa-induced neurochemical changes within the basal ganglia and on levodopa-induced motor alterations in 6-hydroxydopamine-lesioned rats. J. Neurochem. 86, 1328–1337. https://doi.org/10.1046/j.1471-4159.2003.01960.x.
Quiroga-Varela, A., Walters, J.R., Brazhnik, E., Marin, C., Obeso, J.A., 2013. What basal ganglia changes underlie the parkinsonian state? The significance of neuronal oscillatory activity. Neurobiol. Dis. 58, 242–248. https://doi.org/10.1016/j.nbd.2013.05.010.
Ramirez-Zamora, A., Ostrem, J.L., 2018. Globus pallidus interna or subthalamic nucleus deep brain stimulation for Parkinson disease a review. JAMA Neurol. 75, 367–372. https://doi.org/10.1001/jamaneurol.2017.4321.
Redgrave, P., Prescott, T.J., Gurney, K., 1999. The basal ganglia: a vertebrate solution to the selection problem? Neuroscience 89, 1009–1023.
Rosa, M., Fumagalli, M., Giannicola, G., Marceglia, S., Lucchiari, C., Servello, D., Franzini, A., Pacchetti, C., Romito, L., Albanese, A., Porta, M., Pravettoni, G., Priori, A., 2013. Pathological gambling in Parkinson's disease: subthalamic oscillations economics decisions. Mov. Disord. 28 (12), 1644–1652. https://doi.org/10.1002/mds.25427.
Rosenberg, J.R., Amjad, A.M., Breeze, P., Brillinger, D.R., Halliday, D., 1989. The Fourier approach to the identification of functional coupling between neuronal spike trains. Prog. Biophys. Mol. Biol. 53, 1–31.
Rumpel, R., Alam, M., Klein, A., Özer, M., Wesemann, M., Jin, X., Krauss, J.K., Schwabe, K., Ratzka, A., Grothe, C., 2013. Neuronal firing activity and gene expression changes in the subthalamic nucleus after transplantation of dopamine neurons in hemiparkinsonian rats. Neurobiol. Dis. 59, 230–243. https://doi.org/10.1016/j.nbd.2013.07.016.
Ruskin, D.N., Bergstrom, D.A., Walters, J.R., 2002. Nigrostriatal lesion and dopamine agonists affect firing patterns of rodent entopeduncular nucleus neurons. J. Neurophysiol. 88, 487–496. https://doi.org/10.1152/jn.00844.2001.
Schneider, C.A., Rasband, W.S., Eliceiri, K.W., 2012. NIH image to ImageJ: 25 years of image analysis. Nat. Methods 9, 671–675. https://doi.org/10.1038/nmeth.2089.
Shabel, S.J., Proulx, C.D., Trias, A., Murphy, R.T., Malinow, R., 2012. Input to the lateral habenula from the basal ganglia is excitatory, aversive, and suppressed by serotonin. Neuron 74, 475–481. https://doi.org/10.1016/j.neuron.2012.02.037.
Shabel, S.J., Proulx, C.D., Piriz, J., Malinow, R., 2014. Mood regulation.GABA/glutamate co-release controls habenula output and is modified by antidepressant treatment. Science 345, 1494–1498. https://doi.org/10.1126/science.1250469.
Sharott, A., Magill, P.J., Harnack, D., Kupsch, A., Meissner, W., Brown, P., 2005. Dopamine depletion increases the power and coherence of beta-oscillations in the cerebral cortex and subthalamic nucleus of the awake rat. Eur. J. Neurosci. 21, 1413–1422. https://doi.org/10.1111/j.1460-9568.2005.03973.x.
Sharott, A., Vinciati, F., Nakamura, K.C., Magill, P.J., 2017. A population of indirect pathway striatal projection neurons is selectively entrained to Parkinsonian beta oscillations. J. Neurosci. 37 (41), 9977–9998. https://doi.org/10.1523/JNEUROSCI.0658-17-2017.
Smirnov, D.A., Barnikol, U.B., Barnikol, T.T., Bezruchko, B.P., Hauptmann, C., Bührle, C., Maarouf, M., Sturm, V., Freund, H.J., Tass, P.A., 2008. The generation of Parkinsonian tremor as revealed by directional coupling analysis. EPL 83, 20003. https://doi.org/10.1209/0295-5075/83/20003.
Tan, H., Debarros, J., He, S., Pogosyan, A., Aziz, T.Z., Huang, Y., Wang, S., Timmermann, L., Visser-Vandewalle, V., Pedrosa, D.J., Green, A.L., Brown, P., 2019. Decoding voluntary movements and postural tremor based on thalamic LFPs as a basis for closed-loop stimulation for essential tremor. Brain Stimul. https://doi.org/10.1016/j.brs.2019.02.011. pii: S1935-861X(19)30064-6.
Tass, P., Smirnov, D., Karavaev, A., Barnikol, U., Barnikol, T., Adamchic, I., Hauptmann, C., Pawelcyzk, N., Maarouf, M., Sturm, V., Freund, H.J., Bezruchko, B., 2010. The causal relationship between subcortical local field potential oscillations and Parkinsonian resting tremor. J. Neural Eng. 7 (1), 16009. https://doi.org/10.1088/1741-2560/7/1/016009.
Tseng, K.Y., Kasanetz, F., Kargieman, L., Riquelme, L.A., Murer, M.G., 2001. Cortical slow oscillatory activity is reflected in the membrane potential and and spike trains of the striatal neurons with chronic nigrostriatal lesions. J. Neurosci. 21 (16), 9430–9439. https://doi.org/10.1523/JNEUROSCI.21-16-06430.2001.
Vila, M., Périer, C., Féger, J., Yelnik, J., Faucheux, B., Ruberg, M., Raisman-Vozari, R., Agid, Y., Hirsch, E.C., 2000. Evolution of changes in neuronal activity in the subthalamic nucleus of rats with unilateral lesion of the substantia nigra assessed by metabolic and electrophysiological measurements. Eur. J. Neurosci. 12, 337–344. https://doi.org/10.1046/j.1460-9568.2000.00901.x.
Wallace, M.L., Saunders, A., Huang, K.W., Macosko, E.Z., Mccarroll, S.A., Sabatini, B.L., Wallace, M.L., Saunders, A., Huang, K.W., Philson, A.C., Goldman, M., 2017. Genetically distinct parallel pathways in the entopeduncular nucleus for limbic and sensorimotor output of the basal ganglia. Neuron 94, 138. 152.e5. https://doi.org/

10.1016/j.neuron.2017.03.017.
Walters, J.R., Hu, D., Itoga, C.A., Parr-Brownlie, L.C., Bergstrom, D.A., 2007. Phase relationships support a role for coordinated activity in the indirect pathway in organizing slow oscillations in basal ganglia output after loss of dopamine. Neuroscience 144, 762–776. https://doi.org/10.1016/j.neuroscience.2006.10.006.
Winkler, C., Kirik, D., Björklund, A., Cenci, M.A., 2002. L-DOPA-induced dyskinesia in the intrastriatal 6-hydroxydopamine model of parkinson's disease: relation to motor and cellular parameters of nigrostriatal function. Neurobiol. Dis. 10, 165–186. https://doi.org/10.1006/nbdi.2002.0499.